AGU PUBLICATIONS

Tectonics

RESEARCH ARTICLE
10.1002/2015TC004096

Key Points:
- Lithospheric delamination drives transient surface uplifts and subsidences
- Mantle lithosphere rheology controls the dynamics and surface response to lithosphere deformations
- Model results satisfy a number of geological and geophysical observations in the SE Carpathians

Correspondence to:
O. H. Göğüş,
goguso@itu.edu.tr;
oguzgogus@yahoo.com

Citation:
Göğüş, O. H., R. N. Pysklywec, and C. Faccenna (2016), Postcollisional lithospheric evolution of the Southeast Carpathians: Comparison of geodynamical models and observations, *Tectonics*, *35*, 1205–1224, doi:10.1002/2015TC004096.

Received 2 DEC 2015
Accepted 7 MAY 2016
Accepted article online 12 MAY 2016
Published online 21 MAY 2016

©2016. American Geophysical Union. All Rights Reserved.

Postcollisional lithospheric evolution of the Southeast Carpathians: Comparison of geodynamical models and observations

Oğuz H. Göğüş[1], Russell N. Pysklywec[2], and Claudio Faccenna[3]

[1]Eurasia Institute of Earth Sciences, Istanbul Technical University, Istanbul, Turkey, [2]Department of Earth Sciences, University of Toronto, Toronto, Ontario, Canada, [3]Laboratory of Experimental Tectonics, Università Roma TRE, Rome, Italy

Abstract Seismic evidence and thermal and topographic transients have led to the interpretation of lithospheric removal beneath the Southeast Carpathians region. A series of numerical geodynamic experiments in the context of the tectonic evolution of the region are conducted to test the surface-crustal response to lithosphere delamination and slab break-off. The results show that a delamination-type removal ("plate-like" migrating instability) causes a characteristic pattern of surface uplift/subsidence and crustal extension/shortening to occur due to the lithospheric deformation and dynamic/thermal forcing of the sublithospheric mantle. These features migrate with the progressive removal of the underlying lithosphere. Model results for delamination are comparable with observables related to the geodynamic evolution of the Southeast Carpathians since 10 Ma: the mantle structure inferred by seismic tomography, migrating patterns of uplift (>1.5 km) and subsidence (>2 km) in the region, crustal thinning in the Carpathian hinterland and thickening at the Focsani depression, and regional extension in the Carpathian corner (e.g., opening of Brasov basin) correlating with volcanism (e.g., Harghita and Persani volcanics) in the last 3 Myr.

1. Introduction

Small-scale tectonics in response to active and diverse lithospheric deformation in the young Mediterranean orogens motivate intriguing questions about geodynamic driving mechanisms that may be very different from those driving global-scale plate tectonics. Retreating ocean subduction systems in the Mediterranean are widespread, as are zones of back-arc extension [*Le Pichon et al.*, 1981; *Royden et al.*, 1983; *Jolivet and Faccenna*, 2000; *Göğüş*, 2015] and postorogenic lithospheric removal, such as beneath the Apennines-Tyrrhenian [*Channell and Mareschal*, 1989; *Chiarabba and Chiodini*, 2013], Carpathian-Pannonian [*Girbacea and Frisch*, 1998; *Houseman and Gemmer*, 2007], Betic/Rif arc-Alboran [*Docherty and Banda*, 1995; *Platt et al.*, 1998; *Seber et al.*, 1996], Aegean [*Dewey*, 1988; *Jolivet et al.*, 2003], and eastern Anatolian regions [*Göğüş and Pysklywec*, 2008b; *Şengör et al.*, 2008] (Figure 1a). The Mediterranean paleogeographic setting where continental blocks alternate with small oceanic basins favors episodes of subduction and lithospheric thinning (removal). These and many other studies suggest that under certain rheological and boundary conditions (e.g., arc root foundering and postorogenic stage), portions of the lithosphere became gravitationally unstable and subsequently descend into the underlying mantle.

Although a spectrum of lithospheric removal models is possible, two "end-member" geodynamic models have been proposed to account for the distinct surface and crustal features in relation to deep lithospheric removal mechanisms [*Göğüş and Pysklywec*, 2008a]: (1) delamination-type lithospheric removal, where mantle lithosphere (with or without lower crust) peels away from the crust as a coherent slab [*Bird*, 1979], and (2) Rayleigh-Taylor-type viscous convective removal ("dripping" instability model) [*Houseman et al.*, 1981]. Numerical and analogue geodynamical experiments have been conducted to investigate the conditions and controlling parameters for these two processes including the combined style of drip-like delamination [*Conrad and Molnar*, 1997; *Schott and Schmeling*, 1998; *Morency and Doin*, 2004; *Göğüş et al.*, 2011; *Gray and Pysklywec*, 2012; *Stern et al.*, 2013; *Krystopowicz and Currie*, 2013]. Further, a number of studies consider ways in which the surface expression (e.g., topography) and magmatism are modified by lithospheric instabilities [e.g., *Neil and Houseman*, 1999; *Morency and Doin*, 2004; *Pysklywec and Beaumont*, 2004; *Pysklywec and Cruden*, 2004; *Elkins-Tanton*, 2005, 2007; *Göğüş and Pysklywec*, 2008a, 2008b; *Lev and Hager*, 2008; *Pysklywec et al.*, 2010; *Valera et al.*, 2011; *Ueda et al.*, 2012; *Wang and Currie*, 2015].

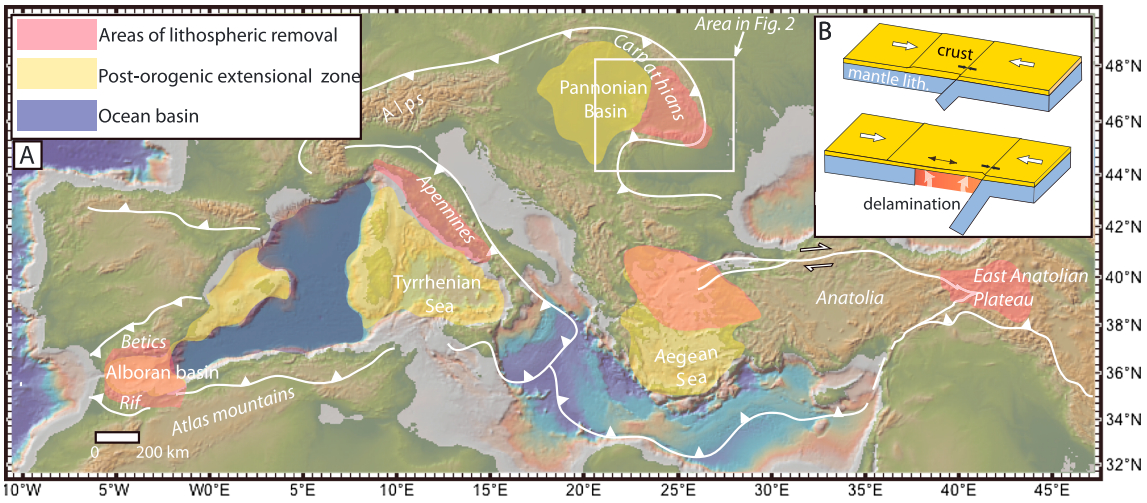

Figure 1. (a) Generalized tectonic map of the Mediterranean region showing regions of lithospheric removal, postorogenic extensional areas, and small ocean basins (references are given in the text). (b) Proposed lithospheric delamination model (migrating instability) where mantle lithosphere with or without lower crust peels off from the upper-middle crust (asymmetric removal).

In this work, we use numerical geodynamical experiments to test the applicability of the lithosphere delamination (migrating instability) model to the postcollisional evolution of the Transylvanian basin and Southeast Carpathians for the last 10 Myr (Figure 1b). Model results are compared to available geological and geophysical constraints of the Southeast Carpathian orogenic region, including the present-day lithospheric structure and surface topographic evolution.

1.1. Tectonic Problem and Significance

The Carpathian Mountains and intra-Carpathian domain/Pannonian Basin represent the easternmost extension of the Alpine orogenic system (Mediterranean Alpides) in central Europe. The later stages of the neotectonic evolution of the Carpathian-Pannonian region are associated with continental collisions of irregular continental fragments such as the Tsia-Dacia (south) and Alcapa (north) microplates and the European plate that occurred in about middle-late Miocene [*Burchfiel*, 1980; *Sandulescu*, 1988; *Schmid et al.*, 2008; *Matenco et al.*, 2007].

Prior to the collision, the Pannonian back-arc basin, a Mediterranean-type back arc, opened (E-W) in response to the eastward retreat of the European ocean plate subduction while the Carpathian orogeny occurred coevally during E-W convergence and the accretion/thrusting of nappes [*Royden et al.*, 1983; *Csontos et al.*, 1992; *Horvarth*, 1993; *Ustaszewski et al.*, 2008]. Since the early Miocene, this subduction resulted in the development of the Carpathian volcanic arc and foreland fold-thrust belts, molasse basins, and flysch deposits [*Burchfiel*, 1980; *Matenco et al.*, 2007].

The focus of this work is on the southeastern section of the Carpathian range (Figure 2). The average peak elevation in the Southeast Carpathians (Vrancea) is $>$1.5 km, and adjacent to the high Carpathians a 13 km deep foreland basin developed (Focsani depression) [*Tarapoanca et al.*, 2003]. Seismic refraction [*Hauser et al.*, 2007] and reflection [*Mucuta et al.*, 2006; *Fillerup et al.*, 2010] studies identify a fundamental tectonic curiosity in this region: thinner crust (35 km thick) exists beneath the Transylvania basin and high Carpathians and is underlain by a low-velocity upper mantle anomaly, while thicker crust (~ up to 46 km) underlies the Focsani basin and is associated with lower surface topography that sits above a NE dipping high-velocity upper mantle seismic anomaly extending from 70 km down to 400 km. The seismological studies are interpreted as showing that the low-velocity upper mantle under the Carpathian hinterland is ascending hot asthenospheric mantle [*Russo et al.*, 2005; *Martin et al.*, 2005; *Ren et al.*, 2012] and the high-velocity anomaly in the foreland—with intermediate-depth seismicity—is a remnant of the previously subducted Vrancea slab [*Fuchs et al.*, 1979; *Oncescu et al.*, 1984; *Wortel and Spakman*, 2000; *Ismail-Zadeh et al.*, 2000; *Sperner et al.*, 2001; *Ren et al.*, 2012; *Bokelmann and Rodler*, 2014]. These observations may suggest that the tectonics in the Southeast Carpathians have been controlled by lithospheric removal under the area.

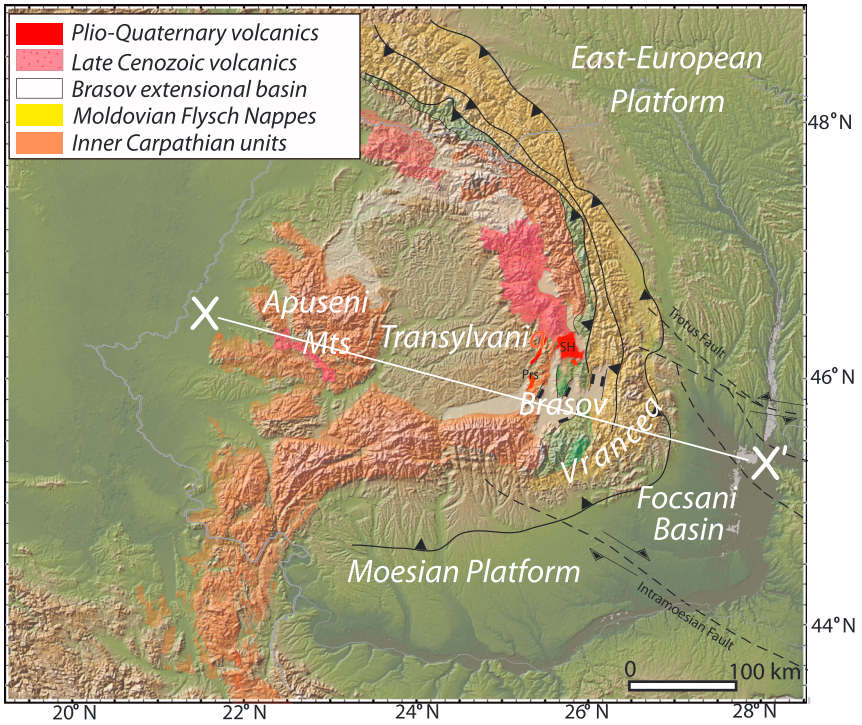

Figure 2. Simplified geological map of Southeast Carpathians showing accreted units, late Cenozoic to present volcanics (Prs = Persani and SH = South Harghita) and extensional Brasov basin. *X-X'* represents the line for lithospheric-scale cross section in Figure 11. See text for sources.

The postulated removal accounts for the high-velocity anomaly as a delaminating (migrating instability) or dripping piece of the continental mantle lithosphere [*Girbacea and Frisch*, 1998; *Sperner et al*., 2004; *Knapp et al*., 2005; *Houseman and Gemmer*, 2007].

The removal of the lower crust and mantle lithosphere from beneath the Southeast Carpathians is also suggested by petrological and geochemical investigations of the 3–0.03 Ma volcanic rocks. According to *Downes et al*. [1995], Pb isotope geochemical analysis from the Persani (Prs) alkali basalts in the southeast corner of the Carpathians (2.5 to 0.7 Ma) suggests that these rocks are derived from an asthenospheric mantle source, akin to ocean island basalts. *Rosenbaum et al*. [1997] and *Harangi et al*. [2006] also suggest that the Persani volcanics are of asthenospheric origin and their magma may have originated from plume-type mantle upwelling under the subduction wedge. The authors postulate that the outpouring of alkaline volcanics postdates the partial melting of subduction-related calc-alkaline magmatism. Corroborating with these interpretations, *Seghedi et al*. [2005, 2011] suggest that the last ~3 Myr of south Harghita volcanism (Sh) was produced by asthenospheric doming due to the postcollisional deformations. Its chemical composition alternates from calc-alkaline to alkaline chemistry where both slab-derived and asthenospheric mantle-derived melts are found in younger volcanics. The transition from calc-alkaline compositions (subduction related) to alkaline magmas in relation to the decompression melting of asthenospheric mantle has been interpreted as a ubiquitous process in the Alpine-Mediterranean region where the mantle lithosphere removal process seems to be widespread. For instance, similar petrological evidence for removal exists at the Betic-Alboran domain [*Turner et al*., 1999; *Duggen et al*., 2005], Aegean Sea-western Anatolia [*Aldanmaz et al*., 2000; *Pe-Piper and Piper*, 2006], and Pannonian Basin-Carpathians [*Harangi et al*., 2006]. See *Lustrino and Wilson* [2007] for more references.

Detailed geological studies indicate regional surface uplift and exhumation above the zone of lithospheric removal and topographic depression adjacent to the inferred removal zone (i.e., Focsani foredeep) (Figure 2). Apatite fission track work by *Sanders et al*. [1999] and *Merten et al*. [2010] indicates that the uplift and exhumation of the Southeast Carpathians and subsidence of the Focsani basin occurred contemporaneously, while a paired uplift and subsidence pattern migrates toward the southeast in conjunction with

the mobilization of the underlying slab [*Leever et al*., 2006; *Matenco et al*., 2007]. Interpretations of crustal-scale seismic images suggest as much as 6 km of sedimentary deposition and southward depocenter migration for the Focsani foredeep basin since the Pliocene [*Leever et al*., 2006]. Subsidence analysis and tectonic interpretations by *Matenco et al*. [2003] and *Bertotti et al*. [2003] postulate that the Focsani basin subsidence rates were a maximum between ~15 and 10 Ma and then decreased slowly since the Pliocene-Pleistocene owing to postorogenic tectonic activity. In agreement with the geological work, geodetic studies conducted by *Van der Hoeven et al*. [2005] indicate 0.25 cm/yr horizontal plate motion toward the southeast (European platform) in the center of the Focsani basin. Moreover, vertical GPS velocities indicate negative anomalies (basin depression) in the Focsani Basin (up to 1 cm/yr) and positive anomalies (surface uplift) of 0.5 cm/yr in the Carpathians. Synthesis of field-oriented geological work and shallow seismic studies suggests that late Miocene-Pliocene surface uplift also occurs to the west of the Carpathian Mountains (e.g., Transylvanian basin) where isostatic uplift may be controlled by sediment unloading through surface erosion or gravitational spreading [*Sanders et al*., 2002; *Krezsek and Bally*, 2006]. *Girbacea and Frisch* [1998] suggest that regional uplift since the Pliocene occurred coeval with the extension and deposition of the Brasov basin in the Carpathian corner following slab break-off and delamination. Overall, the increasing pattern of uplift and subsidence without significant plate shortening/convergence suggests that vertical tectonics due to the inferred lithospheric removal may have played an important role in the neotectonic evolution of the Southeast Carpathians.

The main objective of this work is testing numerical model predictions against geological, geophysical, and petrological interpretations where a number of studies reveal anomalous tectonic displacements in the Southeast Carpathians as a response to postorogenic lithospheric removal. Using a series of high-resolution 2-D thermomechanical numerical experiments, we explore how surface topography and crustal thickness are influenced by the deep lithospheric delamination process following plate collision in the Southeast Carpathians. To address this, we quantitatively investigate deformation styles for a delamination-type lithospheric removal model because an abundance of geological evidence suggests that such process may explain the migratory patterns of surface and thermal transients (i.e., postepisode of subduction, increasing pattern of uplift and subsidence without shortening, and migration of volcanism). Alternatively, viscous dripping-type lithospheric removal can also account for the paired uplift-subsidence pattern in the surface topography but the model predictions may be more applicable for orogens associated with architectural symmetry [*Houseman and Gemmer*, 2007; *Göğüş and Pysklywec*, 2008a; *Lorinczi and Houseman*, 2009].

Slab break-off (detachment) has also been put forward to explain various tectonic anomalies in most of the Mediterranean Alpides, including the Southeast Carpathians [*Nemcok et al*., 1998; *Wortel and Spakman*, 2000; *Sperner et al*., 2001]. Break-off is related to traditional subduction in some cases, but it can also occur during the course of delamination [*Göğüş and Pysklywec*, 2008b]. Therefore, we also explore the effects of the break-off process in the models. We note that the experiments are carried out in two-dimensional space so that the models can treat the lithospheric dynamics in high resolution. However, this is recognized as an approximation to three-dimensional geodynamic processes in the Carpathians.

2. Geological Preconditions, Model Setup, and Material Properties

The numerical code employed here, SOPALE, uses arbitrary Lagrangian-Eulerian finite element techniques to solve for the plane strain deformation of complex viscoplastic materials [*Fullsack*, 1995]. It is based on the arbitrary Lagrangian-Eulerian finite element technique and as such is useful for treating finite deformations and for tracking boundaries (surface and Moho topography) and internal particles (P-T paths) [*Fullsack*, 1995; *Göğüş and Pysklywec*, 2008b]. The configuration of the model is designed as a general representation for the lower crust and gravitationally unstable mantle lithosphere delamination from the upper-middle crust.

2.1. Preconditions for the Gravitationally Unstable Mantle Lithosphere Beneath the Southeast Carpathians

In our experiments, we used a high-density block to initiate delamination as a geological approximation for the Neotethys ocean lithosphere subduction (heavy slab in the system) that transforms into continental delamination after collision (Figure 3). The rest of the mantle lithosphere is denser than the underlying asthenospheric mantle ($\rho_{ml} - \rho_{ast} = 40\,kg/m^3$), and there are two reasons we used such density difference between these layers:

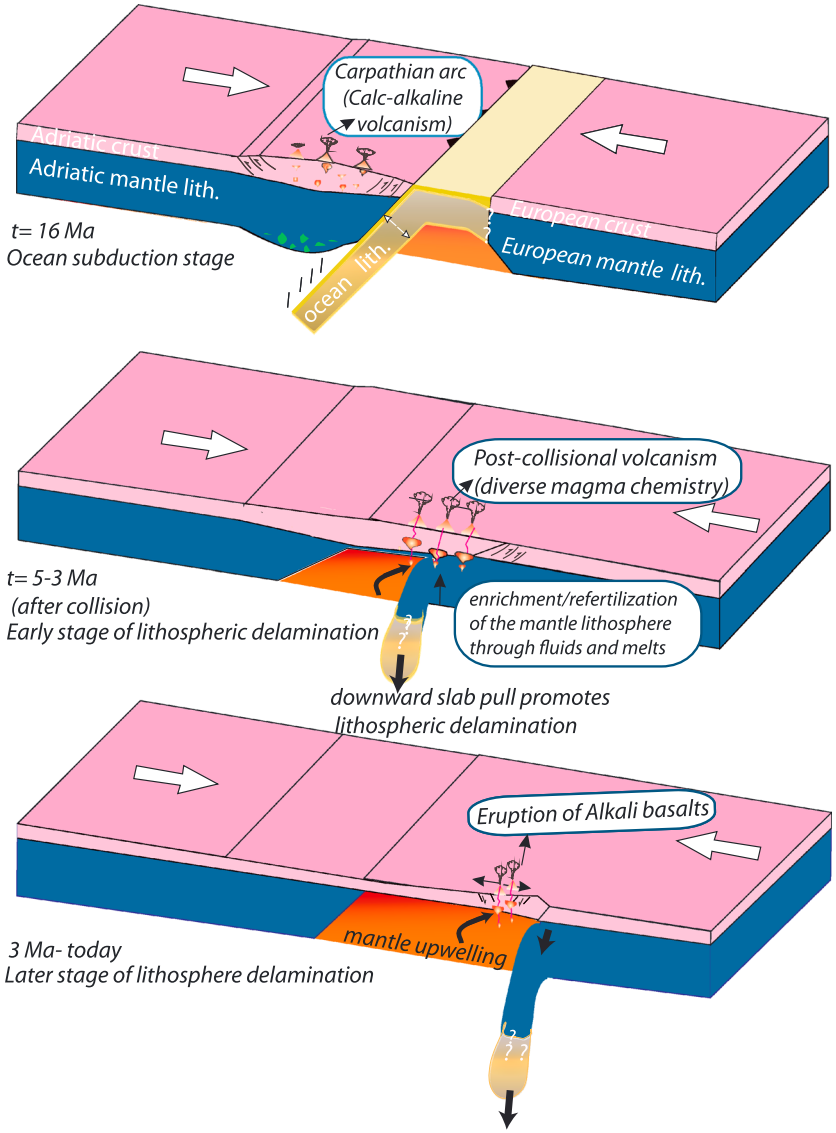

Figure 3. Proposed model for the neotectonic evolution Southeast Carpathians showing the transition from ocean lithosphere subduction to delamination [*Girbacea and Frisch*, 1998; *Knapp et al*., 2005].

1. *The piece of delaminating slab* (*inferred by seismic tomography*) *under the Southeast Carpathians foreland* (*Vrancea region*) *may largely be oceanic rather than continental lithosphere*. Existing geological evidence suggests that the ocean subduction terminated at 11 Ma and "soft collision" occurred between the Tizsa-Dacia microplate and the European plates in conjunction with the peak uplift and 4 km of exhumation [*Burchfiel*, 1980; *Sanders et al*., 1999; *Matenco et al*., 2007]. Though the surface geology suggests the occurrence of late Miocene continental collision (references herein), according to the geological reconstructions, *Royden et al.* [1983] and many others, inferred that high-velocity body—the Vrancea slab—(shown in Figure 3) may largely be an ocean slab rather than a continental lithosphere [*Girbacea and Frisch*, 1998]. Recent seismic tomography work by *Bokelmann and Rodler* [2014] argues that the Vrancea (high-velocity body) sinking/delaminating slab is oceanic lithosphere. Considering the uncertain plate characteristics of the sinking Vrancea slab into the mantle, (i.e., whether it is pulled by the ocean slab or a continental slab), it may be reasonable to interpret that the Carpathians mantle lithosphere is denser than the underlying asthenospheric mantle. According to integrated petrological melt modeling and geophysical interpretations by *Afonso et al.* [2007], the oceanic lithosphere may be ~40 kg/m^3 denser than the underlying mantle.

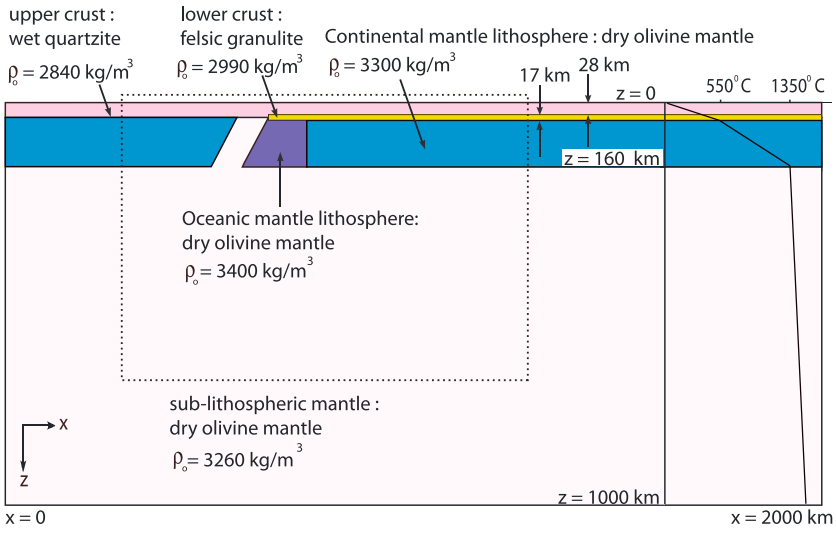

Figure 4. Illustration of model setup for lithosphere delamination model including the dimensions, initial thermal conditions, material types, and density for upper-middle crust, lower crust, mantle lithosphere, and underlying sublithospheric mantle. *X-X'* cross section line in Figure 2 corresponds to the left side (*X*) and right side (*X'*) of the model, respectively.

2. *Progressive refertilization of the mantle lithosphere may have occurred under the Southeast Carpathians by the injection of melts and fluids*. Mantle xenolith studies from the alkali basalts in the Southeast Carpathians by *Vaselli et al*. [1995] and *Rosenbaum et al*. [1997] suggest the enrichment of the mantle lithosphere (metasomatized) by the infiltration of the melts and fluids derived from the upwelling of asthenospheric mantle and the sinking slab. Petrological investigations by *Harangi et al*. [2014] on the young Persani volcanic rocks (mainly alkaline chemistry) are used to account for the asthenospheric mantle origin of basaltic magmas, enriched with Fe and its potential involvement with pyroxenite and eclogite lithology. It is difficult to determine how extensively basaltic melts infiltrated the mantle lithosphere under the region; however, according to recent work by *Zheng et al*. [2015], the lithosphere may be refertilized through decompression melting. They suggest this would make the lithosphere 1.5% denser than the underlying mantle depending on its initial thickness which should be less than $<$150 km. We propose that the initial lithospheric thickness of the Carpathians before the presumed delamination event may not be more than 150 km since the back-arc lithosphere has highly extended ($<$100 km) due to the eastward migration of European subduction. Therefore, based on our estimates for the initial mantle lithosphere density ($\rho_{ml} = 3300$ kg/m^3), a 1.5% density difference is nearly 50 kg/m^3 and our choice of initial density difference (40 kg/m^3) may be in an acceptable range.

2.2. Model Setup and Material Properties

In our models, delamination begins with a 115 km thick and 150 km wide preexisting high-density ocean lithosphere ($\rho_0 = 3400$ kg/m^3, purple) and a gap of sublithospheric mantle under the crust that initiates delamination (Figure 4). This gap permits delamination such that a conduit of weak layer is necessary to allow asthenospheric mantle infiltrate under crust and facilitate delamination [*Bird*, 1979; *Göğüş and Pysklywec*, 2008a]. In these experiments, we considered that a natural conduit of mantle upwelling may occur in a plate collision where a lithospheric-scale fault may be produced.

Figure 4 shows the setup and geometry of the delamination model. Density, ρ, in the model is a function of composition and temperature: $\rho\ (T) = \rho_0\ (1 - \alpha\ (T - T_0))$, where $\alpha = 2 \times 10^{-5}$ 1/K, is the coefficient of thermal expansion, $T_0 = 25$°C is the reference temperature, and ρ_0 is the reference density that depends on material. A series of experiments showed that $\alpha = 3 \times 10^{-5}$ 1/K accelerates the pace of the delamination process less than $t = 1$ Myr; therefore, it has a relatively minor effect in these lithospheric-scale model calculations. In the models, the 160 km thick lithosphere is made up of 28 km thick buoyant upper-middle crust ($\rho_0 = 2840$ kg/m^3, pink), 17 km thick dense lower crust ($\rho_0 = 2990$ kg/m^3, yellow), and 115 km thick dense

Table 1. Rheological Parameters for Reference Experiment EXP-1: Dry Olivine Mantle [*Hirth and Kohlstedt*, 1996], Wet Quartzite Crust [*Gleason and Tullis*, 1995], and Felsic Granulite Crust [*Ranalli*, 1997][a]

	Parameters	Continental Upper-Middle Crust	Continental Mantle Lithosphere	Sublithospheric Mantle	Lower Crust
A	viscosity parameter	1.1×10^{-4} MPa^{-4}/s	4.85×10^{4} MPa$^{-3.5}$/s	4.85×10^{4} MPa$^{-3.5}$/s	8×10^{-3} MPa$^{-3.1}$/s
n	power exponent	4.0	3.5	3.5	3.1
Q	activation energy	223 kJ/mol	535 kJ/mol	535 kJ/mol	243 kJ/mol
φ	effective internal angle of friction	15°–2°	0	0	15°–7°
ρ_0	reference density	2840 kg/m^3	3300 kg/m^3	3260 kg/m^3	2990 kg/m^3
C_m/C_c	plastic yield stress	1 MPa	90 MPa	0	0 MPa
α	coefficient of thermal expansion	2.0×10^{-5} K^{-1}	2.0×10^{-5} K^{-1}	2.0×10^{-5} K^{-1}	2.0×10^{-5} K^{-1}

[a]The physical parameters for the oceanic lithosphere are the same with continental mantle lithosphere, except that its initial density is higher ($\rho_0 = 3400$ kg/m^3) than the continental mantle lithosphere.

mantle lithosphere ($\rho_0 = 3300$ kg/m^3, dark blue) overlying an upper mantle region ($\rho_0 = 3260$ kg/m^3, grey). For rheological calculations we use laboratory measurements based on a viscous flow law of $\dot{\varepsilon} = A\sigma^n \exp\left(\frac{-Q}{RT}\right)$. Here $\dot{\varepsilon}$ is the strain rate, T is temperature, σ is deviatoric stress, and the variables A, n, Q, and R are the viscosity parameter, power law exponent, activation energy, and ideal gas constant, respectively. For continental crust $A = 1.1\times10^{-4}$ MPa^{-4}/s, $n = 4$, and $Q = 223$ kJ/mol are used, based on wet quartzite [*Gleason and Tullis*, 1995]. The wet quartzite rheology is an approximation for the general lithological characteristics of the Transylvanian basin, where nappe stacks of the Southeast Carpathians and the foredeep basin rocks are predominantly made up of sandstone and conglomerate [e.g., *Merten et al*., 2010]. The dense felsic granulite lower crust also represents the weak lower crustal layer where decoupling between the mantle lithosphere and upper-middle crust develops. Such layer is confined in the right side of the model where delamination occurs after crustal thickening due to the plate collision. In addition to the viscous response, the crust and the mantle lithosphere has a brittle Coulomb behavior. For the frictional plastic yield stress a Drucker-Prager yield criterion is used, which is equivalent to the Coulomb criterion in plane strain [*Fullsack*, 1995; *Beaumont et al*., 2006]:

$$\sigma_y = P\sin\phi + Cc \quad (\text{crust})$$

$$\sigma_y = C_m (\text{mantle})$$

For the crust an empirical weakening with the internal angle of friction varying dependent on the strain from $\phi = 15°$–$2°$ (over strain 0.25 to 1.5). Here P is pressure and $\phi = 15°$ is an effective internal angle of friction that implicitly includes the effects of pore fluid pressure Pf in the crust. This is a regular approach in these types/scales of models [e.g., *Pysklywec et al*., 2010; *Gray and Pysklywec*, 2012] in which critical Coulomb wedge studies by *Dahlen* [1984] suggest $\phi = 15°$ for the rocks in the fold-thrust belt of western Taiwan. *Huismans and Beaumont* [2014] estimate that the $\phi = 15°$ for the upper crust at hydrostatic pore pressure conditions.

Furthermore, the crustal weakening employed in these models takes into account the shear zone-related deformations (e.g., cataclastic flow and fault gauges) [*Beaumont et al*., 1996]. The rheological parameters of mantle lithosphere, asthenospheric mantle, and the lower crust for reference model are described in Table 1.

The numerical (width and depth) resolution is 201×101 Eulerian nodes and 601×301 Lagrangian nodes. Half of the Eulerian and Lagrangian elements are concentrated in the top 160 km in order to enhance resolution in the lithosphere. The model has a free top surface, allowing topography to develop as the model evolves. The mechanical boundary conditions at the other three sides are defined by zero tangential stress and normal velocity (i.e., "free slip"). We have extended the depth of the solution space into the lower mantle so that the sinking mantle lithosphere material moves away from the lithosphere. In most of the models we did not impose any plate convergence from the left or right margins of the lithospheric domain because there are only minor far-field boundary stresses (plate shortening) for the Carpathians since the plate collision (~10 Ma). The initial geotherm for the experiments is laterally uniform and is defined by a surface temperature of 25°C, an increase to 550°C at the Moho, an increase to 1350°C at the base of the mantle lithosphere, and an increase to 1525°C at the bottom of the model. The surface and bottom temperatures are held constant throughout the experiments, and the heat flux across the side boundaries is zero. The initial temperature profile is the same in all experiments. Thermal properties (thermal conductivity $k = 2.25$ W/m/K and heat capacity $c_p = 1250$ J/kg/K) are the same for all materials, and we ignore radioactive heat production and shear heating in the model.

Table 2. List of Numerical Experiments Shown in This Work

Experiment	Difference From Reference Model
EXP-1	reference model, $\sigma_y = 90$ MPa
EXP-2	decrease plastic yield stress of the continental mantle lithosphere, $\sigma_y = 30$ MPa
EXP-3	increase plastic yield stress of the continental mantle lithosphere, $\sigma_y = 150$ MPa
EXP-4	impose plate convergence velocity $V_p = 2$ cm/yr
EXP-5	decrease initial lower crustal density to $\rho_0 = 2800$ kg/m^3
EXP-6	decrease initial mantle lithosphere density to $\rho_0 = 3280$ kg/m^3
EXP-7	suppress strain softening for plastic response of the crust $\phi_1 = 15°$ and $\phi_2 = 15°$

3. Model Predictions: The Surface Response to Delamination and Break-Off/Detachment of the Lithosphere

A series of numerical experiments (>100) of continental delamination and break-off were conducted with varying controlling parameters. Here we show a selected group of these experiments that demonstrate how the model behavior changes with modification to some of the primary modeling parameters (Table 2).

3.1. The Reference Experiment, EXP-1 (Delamination and Partial Slab Break-Off)

The reference model EXP-1 has $\sigma_y = 90$ MPa plastic yield stress for the mantle lithosphere, and its geodynamic evolution is shown with plots of surface topography and crustal deformation (Figure 5). We presume that the delamination (subcrustal retreat) begins near the Carpathians suture zone where lithospheric peeling may be a natural progression from retreating ocean subduction after the continental collision [*Göğüş et al*., 2011]. Figure 5a shows that by $t = 5.1$ Myr, the presubducted piece of ocean lithosphere has already broken off and the delamination of the continental mantle lithosphere from the weak lower crust (felsic granulite) has begun. Above the delaminated region, surface topography increases rapidly peaking at 2 km elevation due to the upwelling of the hot-buoyant asthenospheric mantle and isostatic crustal thickening (Figure 5). A portion of the lower crust (shown in yellow) has foundered with the descending mantle lithosphere, and the underlying heavy slab has locally thickened the buoyant upper-middle crust to 40 km by pulling it inward and downward.

As lithospheric delamination progresses, the descending slab is draped forward into the mantle without detaching by $t = 8.9$ Myr. The process is similar to retreating slab subduction with retroplate motion of the delaminating hinge-trench location except that during delamination the continental mantle lithosphere peels away from the crust while allowing mantle flow circulation underneath it (e.g., subcrustal retreat). The replacement of the mantle lithosphere with hot upwelling asthenospheric results in a broader area of positive surface topography ($x = 700$–1000 km) with a surface elevation of more than 2 km. Adjacent to the uplifted region, the surface subsides to -3 km elevation due to the downward pull of the delaminating slab. Note that at this basin location, the underlying upper-middle crust is still relatively thick (~35 km). Conversely, above the zone of delaminated lithosphere, where the surface elevation is positive, the upper-middle crustal thickness is less than 35 km (e.g., $x = 700$–900 km) (Figure 5b).

At $t = 10.1$ Myr, nearly 300 km of mantle lithosphere and lower crust has delaminated from the upper-middle crust and the delaminating slab is necking beneath the hinge location (Figure 5a). The steep hanging slab is yielding at its weakest point at fairly shallow depths (~200 km). Our results are comparable to the numerical results of *Duretz et al*. [2012] and *Magni et al*. [2013] that test the alternating styles of slab detachment and delamination with different rheological properties of the lithosphere after continental collision, and both studies suggest relatively rapid slab detachment at depths ~300 km with appropriate physical conditions. The shallow slab detachment depth also agrees well with the intermediate-depth seismicity of the Vrancea (Southeastern Carpathian loop) earthquakes that occur at the maximum bending location of the slab [*Ismail-Zadeh et al*., 2008] or at the viscous weakening of the dripping mantle lithosphere instability [*Lorinczi and Houseman*, 2009]. A broad region of crust has been exposed to hot, less dense mantle replacement/upwelling, and an area of positive surface topography ($x = 700$–1150 km) develops.

Persistent mantle upwelling produces an enhanced surface topography near the edge of the decoupling zone that reaches a maximum amplitude of ~+3 km of elevation. The high elevation is due to the dynamic and isostatic support, where actively upwelling asthenospheric mantle induces dynamic topography/uplift

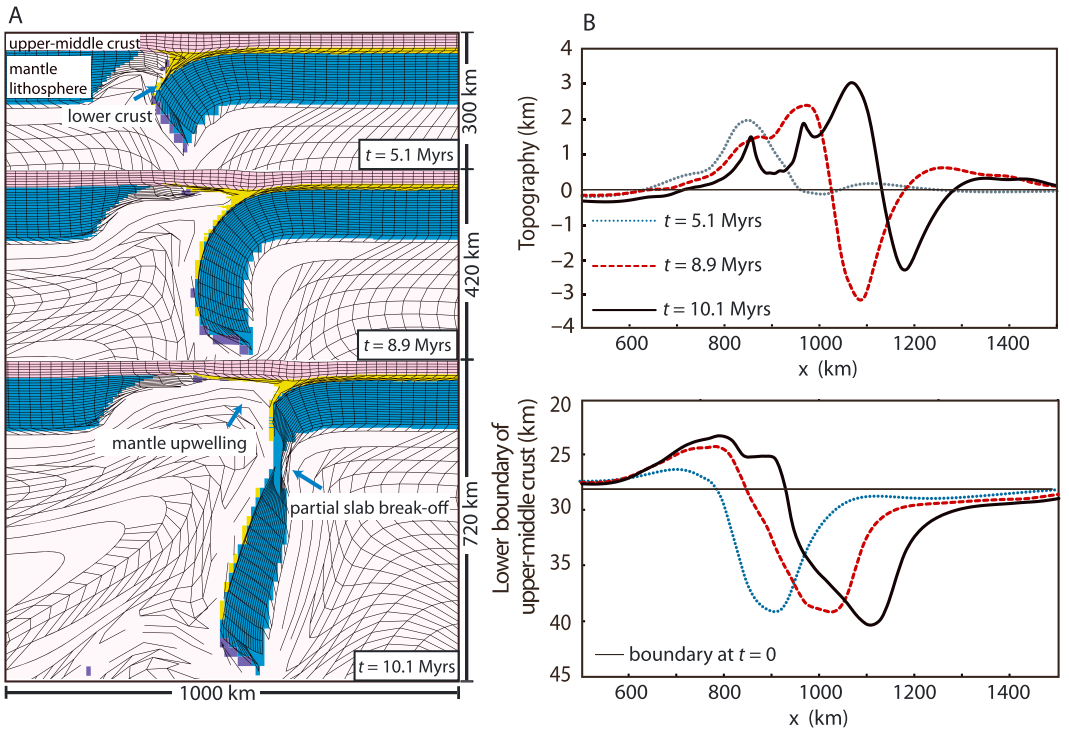

Figure 5. (a) Geodynamic evolution of the reference experiment (EXP-1) where mantle lithosphere with plastic rheology ($\sigma_y = 90$ MPa) and lower crust delaminates. Each frame shows material colors (see Figure 4) and deformed Lagrangian mesh. The latter is plotted at one-half actual resolution; mesh is initially even rectangular. (b) Plots of surface topography and variation of upper-middle crustal thickness at 5.1 Myr, 8.9 Myr, and 10.1 Myr.

and replacement of cold mantle lithosphere with hot asthenosphere and crustal thickening. Next to the high positive peak, negative surface topography (−2 km) develops in response to the downward deflection of the delaminating slab underneath crust. We note that the migratory and transitory pattern of the uplift/subsidence "wave" continues until the end of the delamination. Partial detachment of the delaminating/hanging slab causes the recovery of surface depression to −2 km. At this stage, a region of extension and thinning occurs under the delaminated region between $x = 600$–900 km due to the crustal weakening and stretching by advecting mantle and/or gravitational collapse of the previously thickened-elevated orogenic region.

3.2. EXP-2 (Weaker Mantle Lithosphere)

In an alternate experiment (EXP-2) we explore the surface and crustal response to delamination of a weaker mantle lithosphere where we explore the effects of the slab break-off process in the models ($\sigma_y = 30$ MPa compared to $\sigma_y = 90$ MPa in the previous experiment); in all other respects the model is identical to reference experiment EXP-1. Similar to EXP-1, this experiment begins with a dense subducting block that has been completely detached from the rest of the mantle lithosphere layer, although this occurs 1.2 Myr earlier (Figure 6a). By $t = 5.1$ Myr, the delaminating slab and lower crust dip slightly into the sublithospheric mantle. Inspection of the Lagrangian mesh elements indicates that the rising hot asthenosphere weakens the crust and produces localized stretching between $x = 600$ and 800 km. This upward rise of hot-buoyant mantle creates surface uplift as high as 2 km between $x = 600$ and 1000 km (Figure 6b). Above the delaminating slab, the maximum upper-middle crust thickening is 5 km less than that of the EXP-1, for the same time $t = 5.1$ Myr.

By $t = 8.9$ Myr a small piece of a slab dips into the mantle at a high angle and the mantle flow pattern under the crust develops more symmetrically compared to EXP-1. This is owing to circulating mantle flow that is more confined to the far side of the delaminating margin (lithospheric gap) where downward bending, and therefore the break-off process, of the hanging slab has been delayed. In the zone of delamination, the hot mantle upwelling causes noticeable upper to middle crustal extension and thinning down to

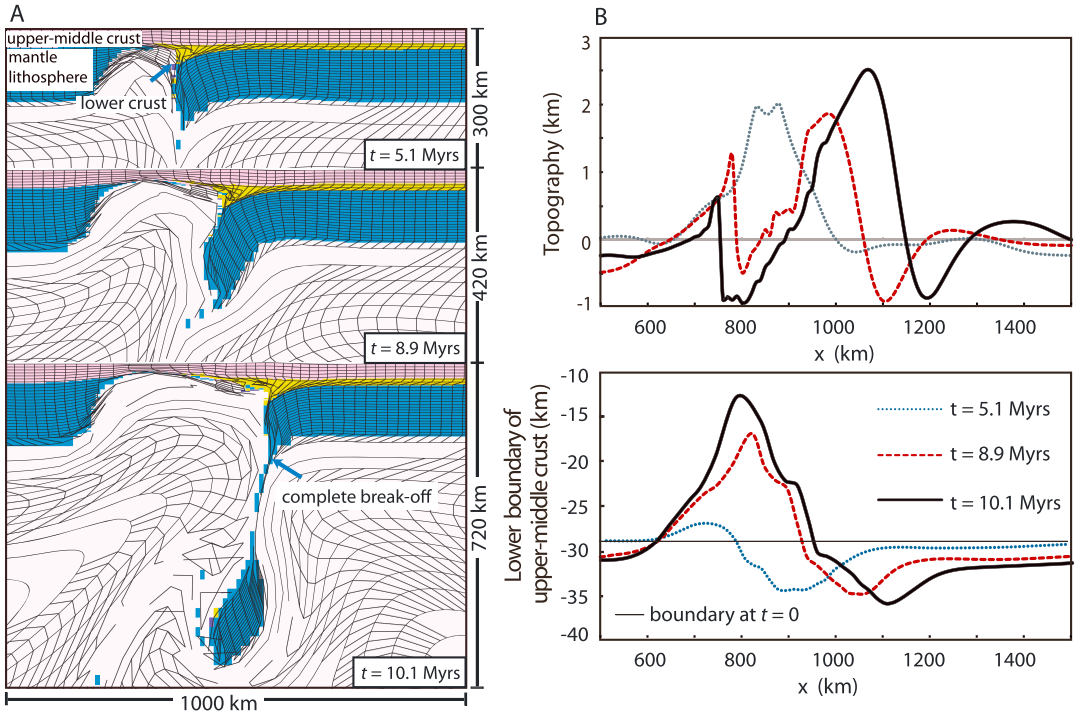

Figure 6. (a) Geodynamic evolution of the experiment (EXP-2) where mantle lithosphere with plastic rheology ($\sigma_y = 30$ MPa) and lower crust delaminates. In all other aspects the model parameters are kept same with the reference experiment (EXP-1). Each frame shows material colors (see Figure 4) and deformed Lagrangian mesh. The latter is plotted at one-half actual resolution; mesh is initially even rectangular. (b) Plots of surface topography and variation of upper-middle crustal thickness at 5.1 Myr, 8.9 Myr, and 10.1 Myr.

20 km crustal thickness and surface subsidence by −500 m. Moreover, the crustal thickening above the delaminating hinge is much less (35 km) than that of reference model at $t = 8.9$ Myr because the hanging piece of slab is smaller.

As delamination evolves, by $t = 10.1$ Myr, a portion of delaminating mantle lithosphere and lower crust has detached and that lithospheric piece descends deeper into the sublithospheric mantle (Figure 6a). The surface expression of this underlying detachment process is minor since there is still ~1 km depression ($t = 8.9$ Myr). Furthermore, at this stage, the underlying mantle dynamics effectively causes significant crustal extension (thinning by more than 15 km) and subsidence above the delaminated zone, whereas the shortening and thickening are still localized above the periphery of the hanging slab (Figure 6b).

3.3. EXP-3 (Stronger Mantle Lithosphere)

EXP-3 was conducted as an alternative end-member experiment where the yield stress of the mantle lithosphere is increased to $\sigma_y = 150$ MPa (Figure 7), in which the effects of the potential slab break-off in the course of delamination are removed. Figure 7a shows that with a higher strength of the mantle lithosphere, the propensity of the mantle lithosphere to detach from the crust is reduced. This significantly changes the surface topographic response. Slab bending is more pronounced because the lengthy slab continues curving until it reaches its yield stress (Figure 7a). By $t = 5.1$ Myr, the delaminating slab and lower crust deflect the crust downward under the hinge zone resulting in 1 km of surface subsidence and thickening of more than 40 km (Figure 7 b). At the delamination zone, more than 1.5 km of surface topography develops above the upwelling sublithospheric mantle. In this experiment, the paired subsidence and uplift that develop in response to deep lithospheric delamination are similar to the reference experiment but subsidence and shortening/thickening in the delaminating margin (~40 km) is amplified since the stronger slab pulls the crust down more vigorously.

Figure 7b shows that by $t = 8.9$ Myr, the delaminating mantle lithosphere and lower crust dip ~90° into the mantle as an intact plate/slab. This strong hanging slab is attached to the crust and produces negative surface

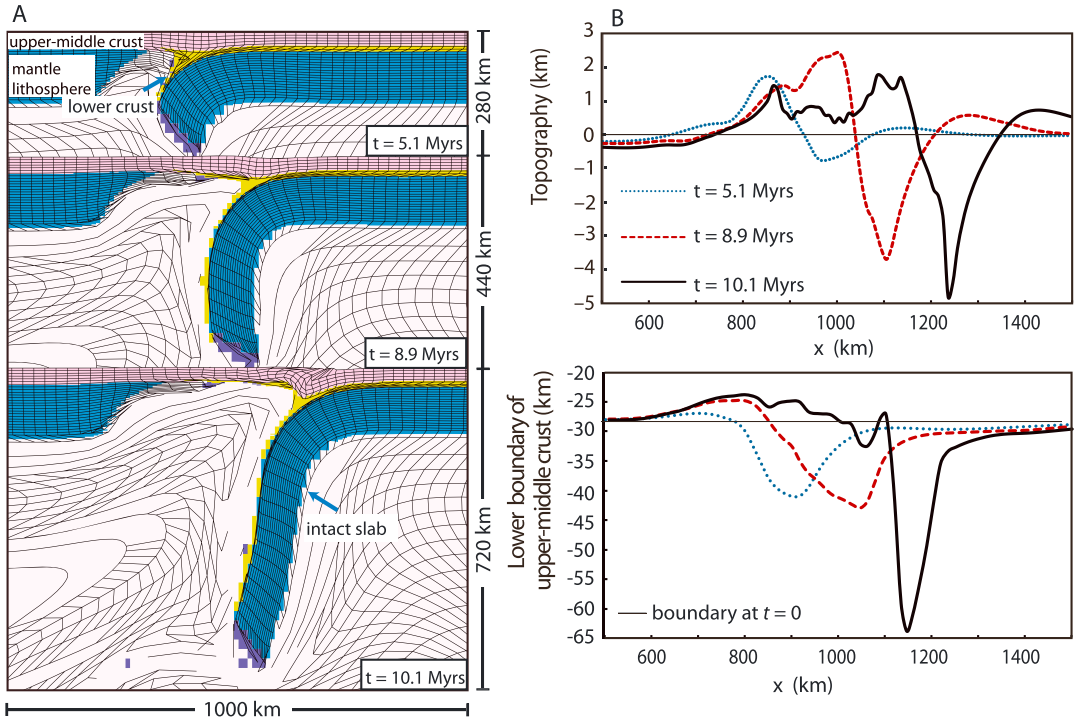

Figure 7. (a) Geodynamic evolution of the experiment (EXP-3) where mantle lithosphere with plastic rheology ($\sigma_y = 150$ MPa) and lower crust delaminates. In all other aspects the model parameters are kept same with the reference experiment (EXP-1). Each frame shows material colors (see Figure 4) and deformed Lagrangian mesh. The latter is plotted at one-half actual resolution; mesh is initially even rectangular. (b) Plots of surface topography and variation upper-middle crustal thickness at 5.1 Myr, 8.9 Myr, and 10.1 Myr.

deflection to nearly −4 km as well as crustal thickening up to 45 km. The surface topography at the delamination front has increased to more than 2 km because the mantle uprising increases elevation in conjunction with the crustal thickening induced by the slab pull.

At $t = 10.1$ Myr, delaminated lithosphere from the overlying crust has retreated ~250 km compared to $t = 5.1$ Myr and it has not detached from the surface lithosphere. A very broad region of positive surface topography develops above the zone of delaminated lithosphere ($x = 750$–1150 km), although the crust has been thinned in most places (e.g., $x = 600$–1000 km). On the other hand, the crust has been anomalously thickened-shortened (to nearly 65 km) above the hinge zone as the strong (undetached) mantle lithosphere also causes substantial subsidence to 5 km. These model results show topographic anomalies that migrate (similar to the reference model) but are accompanied by more crustal thickening and subsidence. We interpret these results to indicate that surface uplift is not persistent during underlying slab migration because extension is more distributed due to the collapse of a previously thickened and thermally weakened crust heated by the mantle upwelling (Figure 7b).

3.4. EXP-4 (Impose Convergence Velocity of $V_p = 2$ cm/yr)

In previous experiments, we did not consider the effects of a plate convergence velocity imposed on the lithospheric domain since the horizontal forcing in the southeastern Carpathians significantly slowed after the plate collision occurred about 10 Ma [*Matenco et al.*, 2007]. For experiment EXP-4 we applied a convergence velocity $V_p = 2$ cm/yr along the right side of the lithospheric plate boundary, to investigate the role of orogenesis (horizontal tectonics) in the course of the delamination (vertical tectonics) process. In this configuration, the left margin of the lithosphere is held fixed, and a small outward flux, v_x, is distributed evenly along the sides of the sublithospheric mantle to balance the mass of injected lithosphere. In all other aspects the model parameters are kept same with the reference experiment (EXP-1). Figure 8a shows the geodynamic evolution of the experiment after $t = 5.1$, 8.9, and 10.1 Myr. The early stages of the experiment develop similar to the reference experiment: the delaminating mantle lithosphere slab and the lower crust

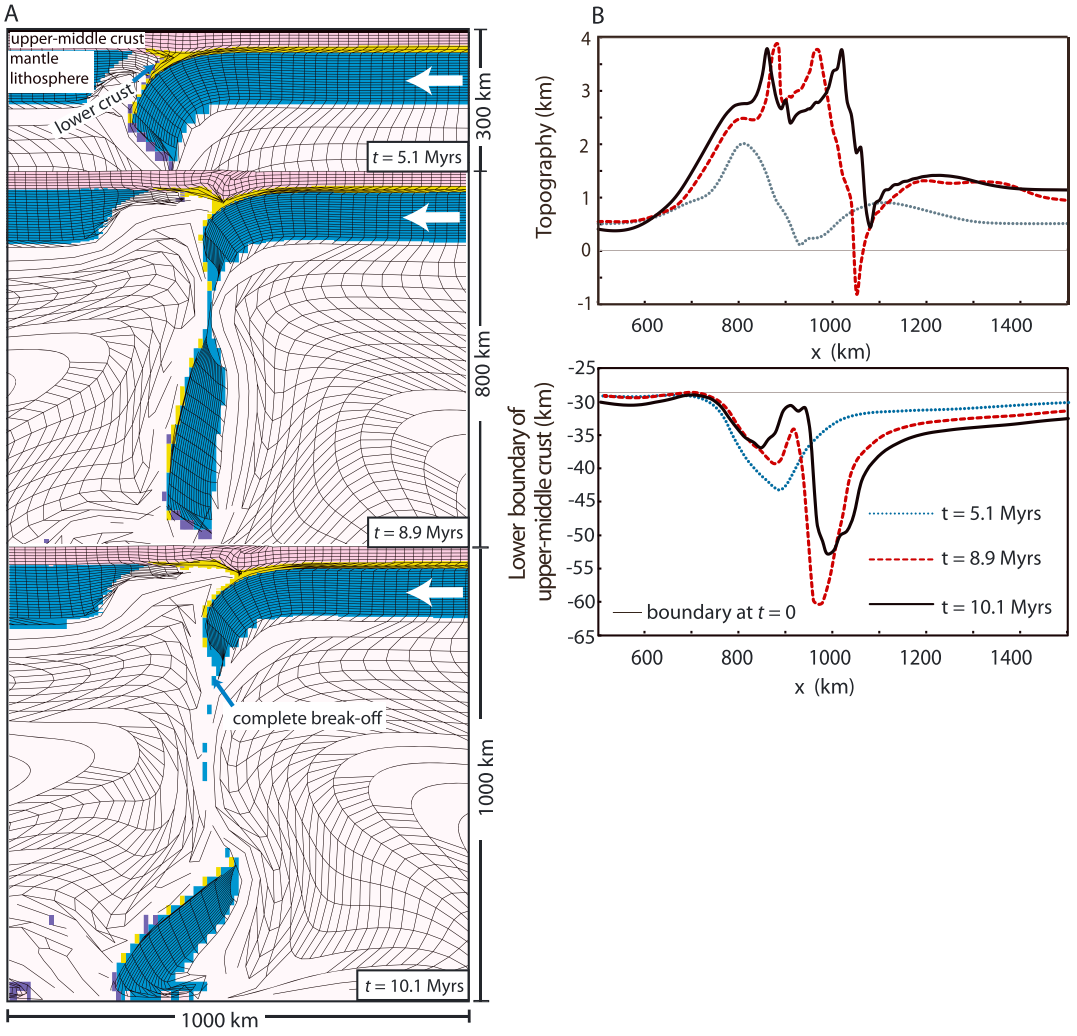

Figure 8. (a) Geodynamic evolution of the experiment (EXP-4) where convergence velocity (V_p = 2 cm/yr) along the right side of the lithospheric plate boundary is imposed. In all other aspects the model parameters are kept same with the reference experiment (EXP-1). Each frame shows material colors (see Figure 4) and deformed Lagrangian mesh. The latter is plotted at one-half actual resolution; mesh is initially even rectangular. (b) Plots of surface topography and variation upper-middle crustal thickness at 5.1 Myr, 8.9 Myr, and 10.1 Myr.

sink to the less dense sublithospheric mantle while peeling off from the upper-middle crust. The applied horizontal plate convergence provides additional forcing to the edge of the sinking (delaminating) lithosphere; therefore, the hanging slab steepens more rapidly compared to the reference experiment.

By t = 8.9 Myr, (after nearly 82 km of delaminating hinge migration) the hanging slab detaches at a relatively shallow lithospheric depth of $<$200 km. Because the lithosphere shortens and thickens due to the applied convergence, positive surface topography $>$500 m dominates the model domain. The maximum elevation reaches more than 3.5 km, induced by mantle upwelling contemporaneous with plate shortening (Figure 8b). At x = 1100 km a surface subsidence down to $-$1 km develops as a response to the slab pull. The magnitude of this subsidence is less compared to the reference experiment at a similar stage of evolution, owing to the plate shortening. Crustal thickness varies from 29 km at the left edge of the model to 60 km where the slab is being pulled downward.

By t = 10.1 Myr, the hanging lithosphere completely detaches from the rest of the lithospheric slab and the detached portion reaches to the bottom of the solution box. At this time only a small amount of lithosphere delaminates with respect to the previous time (t = 8.9 Myr) and the migration of the delaminating hinge (the locus of decoupling between the upper-middle crust and the mantle lithosphere) is 125 km less compared to

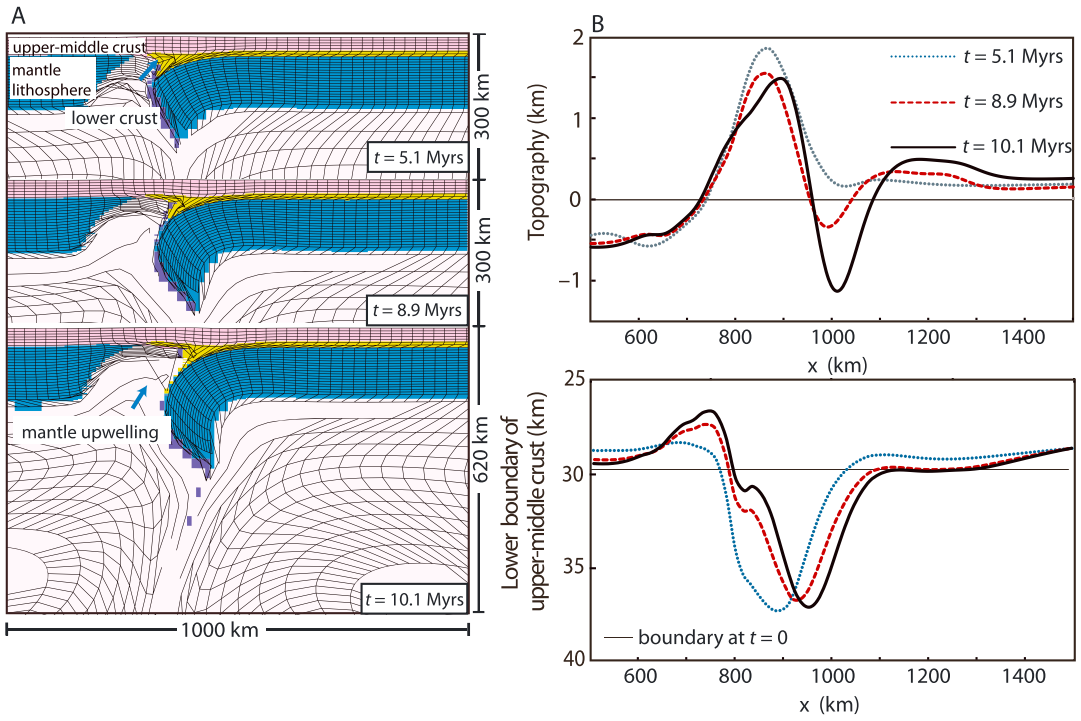

Figure 9. (a) Geodynamic evolution of the experiment (EXP-5) where initial lower crustal density is decreased to $\rho_0 = 2800$ kg/m^3. In all other aspects the model parameters are kept same with the reference experiment (EXP-1). Each frame shows material colors (see Figure 4) and deformed Lagrangian mesh. The latter is plotted at one-half actual resolution; mesh is initially even rectangular. (b) Plots of surface topography and variation upper-middle crustal thickness at 5.1 Myr, 8.9 Myr, and 10.1 Myr.

the reference experiment. Models show that the imposed plate convergence yields an earlier development of slab break-off than the reference experiment, and the same effect also hinders the occurrence of broader areas of lithosphere delamination where plateaus may form. These predictions are consistent with laboratory-based experiments that considered the geodynamic evolution of orogens from subduction to continental delamination [*Göğüş et al*., 2011]. Namely, analogue models with higher rates of imposed convergence show less propensity for delamination and favor crustal accretion to the overriding plate. At the last stages of this experiment, there is not much change in terms of surface topography and crustal thickening compared to $t = 8.9$ Myr except that the crust rebounds to +1 km surface elevation and the crustal thickness reaches 50 km due to the gradual cessation of downwelling forces created by the deeper sinking lithosphere.

3.5. EXP-5 (Decrease Initial Lower Crustal Density to $\rho_0 = 2800$ kg/m^3)

To consider the influence of the lower crustal density in the lithosphere delamination/break-off system, we conduct model with decreased initial density of the lower crust $\rho_0 = 2800$ kg/m^3 for EXP-5 (otherwise all other parameters are kept same with the reference experiment EXP-1). By making the lower crust more buoyant, we tested how much surface elevation varies, though it is pulled down by the gravitationally unstable mantle lithosphere. Figure 9a shows that at $t = 5.1$ Myr there is less sinking/delaminating slab into the sublithospheric mantle compared the EXP-1. The surface response to the decreased lithospheric forces is a more subdued surface subsidence and crustal thickening, but the amount of surface uplift (~2 km) due to the mantle upwelling (isostatic + dynamic compensation) is very close with the reference model (Figure 9b). Overall, a decreased lower crustal density suppresses the delamination process and by $t = 8.9$ Myr there has been only ~40 km delaminating hinge migration while the negative surface topography develops only above the sinking slab. Figure 9a shows that by $t = 10.1$ Myr, compared to the reference experiment (EXP-1) the hinge migration is 160 km less (i.e., less delamination occurs with reduced crustal density). This also reflects the development of narrow region of positive surface elevation where sublithospheric mantle rises (between $x = 730$–960 km), and adjacent to this the surface subsides down to −1 km. In this experiment, because there is a smaller slab attached to the crust, the crust does not thicken as much as the reference experiment since the shortening in these experiments without plate convergence is largely controlled by the downward slab pull impact on the crust.

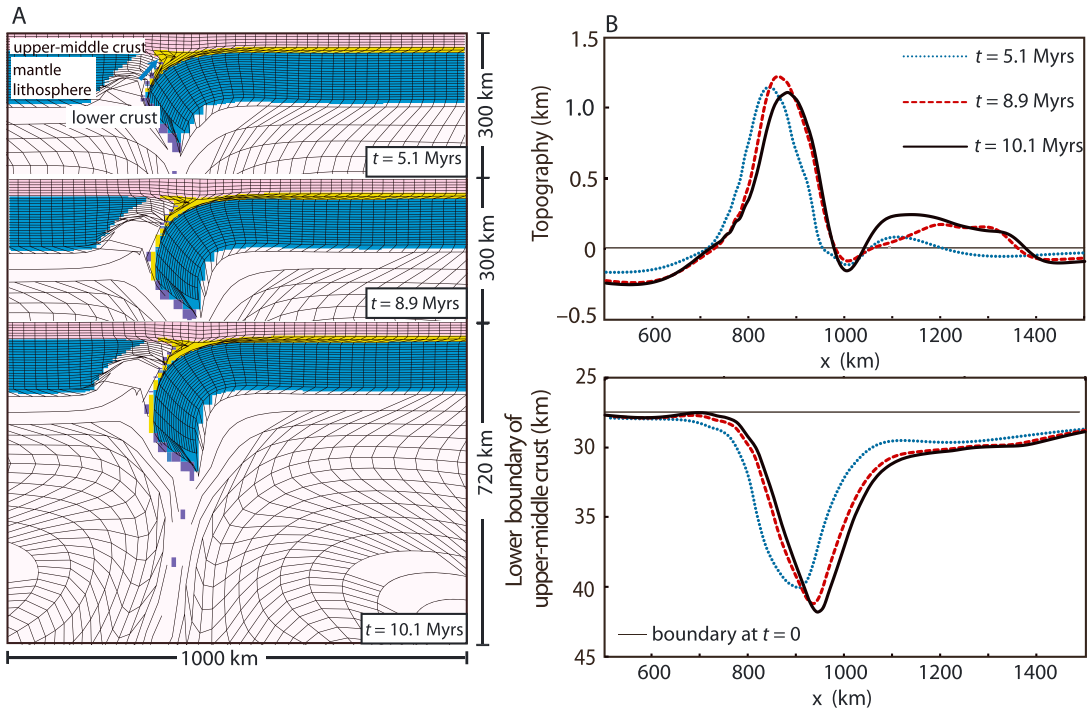

Figure 10. (a) Geodynamic evolution of the experiment (EXP-6) where initial mantle lithosphere density is decreased to $\rho_0 = 3280\ kg/m^3$. In all other aspects the model parameters are kept same with the reference experiment (EXP-1). Each frame shows material colors (see Figure 4) and deformed Lagrangian mesh. The latter is plotted at one-half actual resolution; mesh is initially even rectangular. (b) Plots of surface topography and variation upper-middle crustal thickness at 5.1 Myr, 8.9 Myr, and 10.1 Myr.

3.6. EXP-6 (Decrease Initial Mantle Lithosphere Density to $\rho_0 = 3280\ kg/m^3$)

The buoyancy difference between the lithosphere and the underlying sublithospheric mantle can have a significant impact on the evolution of lithosphere delamination process. In this experiment (EXP-6), we used the same modeling parameters with the reference experiment (EXP-1) but set the initial density of the mantle lithosphere to $\rho_0 = 3280\ kg/m^3$ ($20\ kg/m^3$ less dense than EXP-1); therefore, we test how much delamination (removal) occurs with less density difference. EXP-6 shows that such a decrease in mantle lithosphere density (and hence density contrast between lithosphere and sublithospheric mantle) reduces the pace of the evolution of the lithospheric delamination/break-off system. The effects are minor during the early stages of the experiment, but by $t = 8.9$ Myr, there is at least 80 km less delaminating hinge migration compared with the reference experiment (Figure 10a). Throughout the experiment, the lithospheric removal process and the resulting mantle upwelling-replacement occurs in a more limited zone (between $x = 700$ and ~1000 km), in which positive surface topography develops (Figure 10b). The lithosphere delamination does not progress much by $t = 10.1$ Myr. A piece of hanging lithosphere is attached to the overlying crust, and the surface basin driven by the slab pulling is only couple of hundred meters deep at $x = 1000$ km. Clearly, the slab pull forcing induced by the more buoyant hanging slab in EXP-6 is reduced compared to the reference model.

3.7. EXP-7 (Suppress Strain Softening for Plastic Deformation of the Crust)

In experiment EXP-7, we turned off the weakening of the upper-middle crust (wet quartz) by setting $\phi 1 = 15°$ and $\phi 2 = 15°$ to investigate the response of a relatively stronger crust to lithosphere delamination without enhanced crustal weakening (i.e., by the pore fluid pressure and significant shear zone development) (Figure 11). The development of delamination and the corresponding crustal thickness and topography in every stage of the experiment are almost same with the reference experiment. However, by $t = 10.1$ Myr, the surface subsidence and crustal thinning did not occur at $x = 900$ m as in the reference experiment. This is because the stronger crust resisted crustal weakening and a local surface depression did not develop as a response to heating through mantle upwelling and weakening of the crust. As such in considering the evolution of the orogen in the Southeast Carpathians—from the Apuseni Mountains to the Focsani foreland

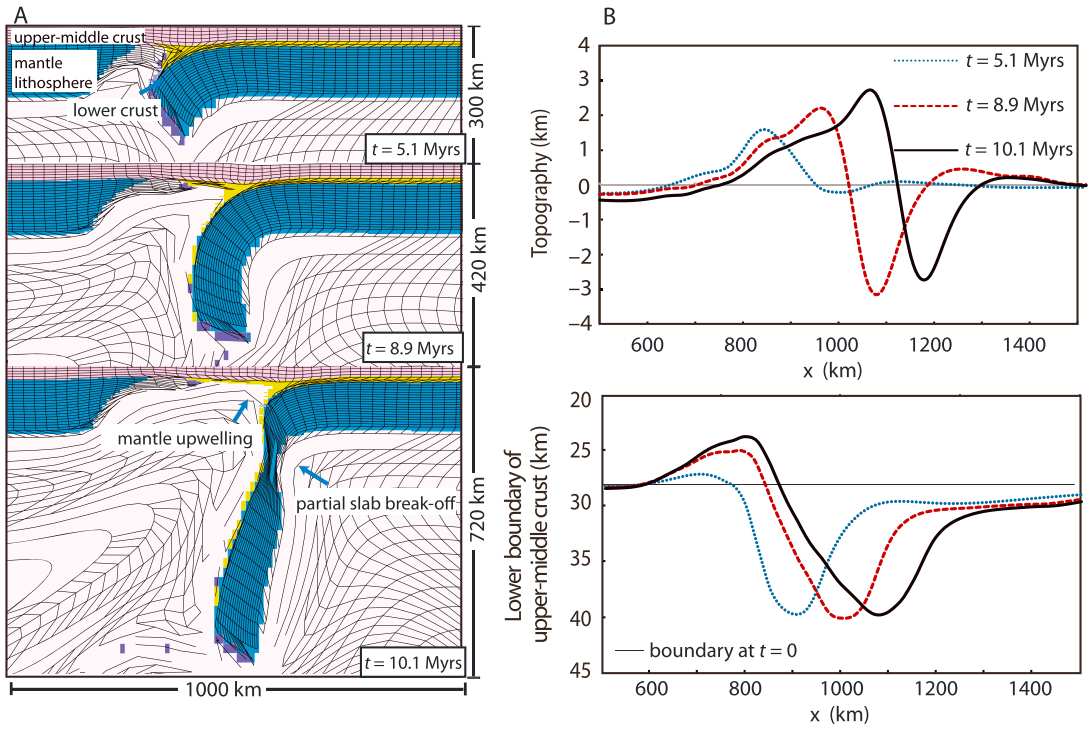

Figure 11. (a) Geodynamic evolution of the experiment (EXP-7) where plastic strain softening of the crust is supressed $\varphi_1 = 15°$ and $\varphi_2 = 15°$. In all other aspects the model parameters are kept same with the reference experiment (EXP-1). Each frame shows material colors (see Figure 4) and deformed Lagrangian mesh. The latter is plotted at one-half actual resolution; mesh is initially even rectangular. (b) Plots of surface topography and variation upper-middle crustal thickness at 5.1 Myr, 8.9 Myr, and 10.1 Myr.

basin—the results of the reference experiment (with crustal weakening imposed) may be more consistent with the opening of the Brasov extensional basin in the Carpathians hinterland.

4. Comparison of Model Results Against Observations

Our model results show that vertical displacements (with paired surface uplift and subsidence) develop in response to the delamination and subsequent detachment of lithosphere and that the presence or absence of slab detachment can alter this surface response. Model predictions also show that the localized crustal deformations (extension/basin formations) are also dependent on the strength of the crust. The spatially varying topographic anomalies and crustal deformation are consistent with many of the observations of the surface tectonics and crust-mantle structure observed in the Southeast Carpathians.

Figure 12a shows the reference delamination experiment (EXP-1) results for upper-middle crustal thickness variation at $t = 10.1$ Myr (i.e., in this comparison this stage is considered "present day"). The model results are compared against the observed crustal thickness (with and without lower crust) data derived by seismological studies [e.g., *Hauser et al.*, 2007] (Vrancea 2001 V_p model). According to *Hauser et al.* [2007], the observed thickness of the upper-middle crust varies from 26 to 30 km from the Apuseni to Carpathian Mountains (plate hinterland) and this is in good agreement with the model result in which the thickness of the upper-middle crust is between 24 to 30 km in the same area where lower crust and mantle lithosphere have probably delaminated. These seismological studies show that there is 30 km thick upper-middle crust under the Focsani basin where topography is at least 1.5 km lower than the high elevation in the Carpathians. The modeled thickness of the upper-middle crust increases (to as thick as 40 km) in the same location, and it becomes thinner toward the eastern end of this basin. A similar pattern of crustal thinning under the hinterland and thickening in the foreland (to 45 km) is proposed for the Moho topography estimates by *Hauser et al.* [2007] and also *Fillerup et al.* [2010]. The approximations made for the upper-middle crustal thickness match well with the estimates (especially under the hinterland domain) because the models presumed lower crustal removal in the same region due to a delamination process. Reconciling the model

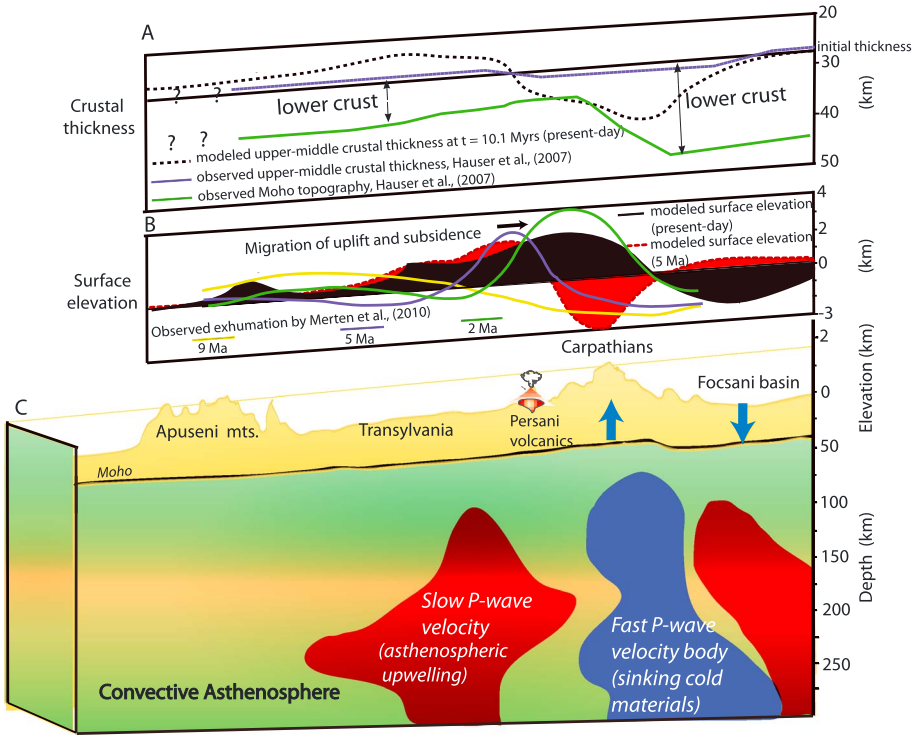

Figure 12. (a) Modeled crustal thickness for the reference experiment at $t = 0$ and $t = 10.1$ Myr (present day) and the observed upper-middle crustal thickness. Moho topography estimates by *Hauser et al.* [2007]. (b) Modeled surface elevation at present day and 5 Ma. Observed crustal exhumation by *Merten et al.* [2010] is shown in the same plot for 9 Ma, 5 Ma, and 2 Ma. (c) Upper mantle-scale NW-SE cross section (down to 300 km depth) inferred from *P* wave tomography model by *Ren et al.* [2012]. The marked fast and slow velocities correspond to ± 2%. Moho topography estimates by *Hauser et al.* [2007] and *Fillerup et al.* [2010]. Please see Figure 2 for the orientation of the profile (present-day surface elevation is shown including main geological features from the Apuseni Mountains to Focsani basin).

results with observations suggests that the higher elevation of the Carpathian Mountains (>1.5 km) and the uplift of Transylvania may not fully be compensated by thicker crust but also by replacement of the hot mantle after lithosphere delamination in which slow seismic velocity anomalies are also observed (Figure 12c) [*Russo et al.*, 2005; *Martin et al.*, 2005; *Ren et al.*, 2012]. Also, the subsidence at the Focsani foredeep basin —with up to 10 km of sediment deposition and underlain by thickened crust—may be due to dynamic subsidence driven by the descent of the existing slab [*Fuchs et al.*, 1979; *Oncescu et al.*, 1984; *Wortel and Spakman*, 2000; *Ismail-Zadeh et al.*, 2000; *Sperner et al.*, 2001; *Ren et al.*, 2012; *Bokelmann and Rodler*, 2014]. We also interpret that the modeled crustal stretching, caused by the hot mantle upwelling after delamination (i.e., especially at highest crustal thinning down to ~25 km), may correspond to the opening of the Pliocene age Brasov extensional basin [*Girbacea and Frisch*, 1998]. This would also be correlated with the asthenospheric mantle-derived outpouring of Persani and south Harghita volcanics (since 3 Ma) in the Carpathians loop [*Downes et al.*, 1995; *Rosenbaum et al.*, 1997; *Seghedi et al.*, 2005, 2011].

In Figure 12b, we show the model predictions of surface elevation change from the reference experiment at $t = 5.1$ Myr and $t = 10.1$ Myr, (given in Figure 12b as 5 Ma for the former and present day for the latter) from the Apuseni Mountains to the Focsani basin. In the same plot, we also show the postcollisional evolution of exhumation tectonics in the same region derived by thermochronological data from *Merten et al.* [2010]. According to their work, the magnitude of the crustal exhumation and shortening along the thrust nappes increases toward the Focsani foreland basin. Namely, up to 1 km of exhumation occurred following the collision at the Transylvania region at about 9 Ma. Subsequently, at 5 Ma the recorded maximum exhumation has migrated toward the foreland and nearly 3 km of exhumation occurred at the Carpathian nappes as a response to the crustal shortening. At the very last stage of the exhumation process, since the Pliocene, up to 4 km of crustal exhumation has been suggested at the present-day position of the Carpathian

Mountains. Coeval with this migrating exhumation, the Focsani basin depocenter has moved to the south with increasing sediment deposition [*Leever et al*., 2006]. The surface topography evolution of the reference experiment (EXP-1) shows that there is a migration of the paired uplift and subsidence as a response to the lithosphere delamination and break-off (Figure 5b) and the magnitude of vertical displacements is comparable to the amount of crustal exhumation estimated by *Merten et al*. [2010]. We suggest that EXP-1's results are consistent with the surface response to a lithosphere delamination that begins under the Carpathians hinterland (Figure 12c). Here the maximum elevation increases over time owing to the loss of the underlying slab, the thermal and dynamic effects of mantle replacement under the crust, and accompanying isostatic thickening. For instance, in Figure 12b, at 5 Ma ($t = 5.1$ Myr) the 2 km of model surface uplift may correspond to the documented 3 km of crustal exhumation that occurred in the Carpathians corner about 5 Myr ago. While thermochronological data indicate that crustal burial (nearly 2 km) occurred in the Carpathians at that time (5 Ma), 3 Myr later 4 km of crustal exhumation has been inferred [*Merten et al*., 2010]. Such exhumation is comparable with the 3 km uplift of the surface topography from −3 km elevation in the model.

5. Conclusions

We conducted numerical experiments to investigate the time-dependent surface and crustal response to delamination-type lithospheric removal (lower crust and mantle lithosphere) processes and slab break-off in a postcollisional tectonic environment. The results show progressive upwelling of the asthenospheric mantle accompanied by thinning of the overriding crust and increasing surface elevations. At the same time, downwelling forces related to the sinking and delaminating mantle produce localized crustal thickening and subsidence above the delaminating hinge (e.g., ~−2 km). These effects migrate through time as lithospheric delamination progresses. The results demonstrate that mantle dynamics can play a major role in the evolution of surface tectonics and topography in response to delamination.

We have shown that the rheological characteristics of the mantle lithosphere control the dynamics of lithosphere delamination as well as the surface impact of slab break-off. For example, lithospheric delamination experiments with a weaker mantle lithosphere yield a complete slab detachment after the delamination. As a result the downwelling force is reduced and this causes a decrease in the magnitude of crustal thickening and subsidence under the delaminating margin. Stronger mantle lithosphere delamination induces more localized crustal thickening above the delamination hinge and a broader zone of extension and uplift that occurs over the region of mantle upwelling. When a lithospheric convergence velocity is imposed, the slab break-off occurs earlier and the surface experiences higher uplift of a broad plateau-type region. A decrease of the density of the lower crust and mantle lithosphere both suppress the mantle lithosphere delamination process as well as the associated surface response. With a stronger crust (viz., without the ability to strain soften), delamination of the mantle lithosphere continues, but there is a reduced propensity for the crust to extend and subside above the removed lithosphere.

Our numerical results help interpret observations of topography, crustal thickness, crustal exhumation, and mantle structure of the Southeast Carpathians: (1) the geodynamic evolution of the lithosphere delamination is consistent with the proposed seismic tomography interpretations beneath the region; (2) positive (+) and negative (+) surface topography that migrates with the delaminating lithosphere is consistent with the observed migration and increasing amount of crustal exhumation by *Merten et al*. [2010] and basin depocenter by *Leever et al*. [2006] from Transylvania to the Focsani foreland basin; (3) predicted thinner crust at the Carpathians hinterland (higher elevation) and thicker crust at the Focsani depression (lower elevation) are in good agreement with the seismologically observed crustal thickness from *Hauser et al*. [2007]; and (4) extension/thinning in the models is in agreement with the opening of young extensional basin in the Carpathian corner (e.g., Brasov basin) and the volcanism in the last 3 Myr (i.e., Persani and south Harghita volcanics) derived from asthenospheric mantle origins. Although the model results suggest a reasonable approximation for the geodynamics of the Southeast Carpathians, our motivation was not to simulate the entire complex evolution of the region. Rather, the works provide a reference frame for understanding how a delamination removal process can account for the results; future refinement to the models and observations would help improve these comparisons and interpretations. Finally, we suggest that while this research focuses on the late Cenozoic geodynamic evolution of Southeast Carpathians, the outcome of this

work may have general implications for the evolution of other Mediterranean-type orogenic regions (e.g., Apennines, Betics, and the Anatolian Plateau) where compelling documentation on lithospheric delamination—following retreating subduction—has been interpreted through a range of geophysical, geological, and petrological observations.

Acknowledgments

The project was conducted while O.H.G. was a PDF with Greg Houseman at the University of Leeds. O.H.G. acknowledges support from NERC and fruitful discussions with the members of the South Carpathian Project Working Group. R.P. is grateful for funding from an NSERC Discovery Grant. O.H.G. and R.P. also acknowledge support from the TUBITAK 2221 Visiting Scientist Program for facilitating collaboration for the work. The paper was improved by constructive reviews from Linda-Elkins Tanton, Claire Currie, and an anonymous reviewer. Leigh Royden provided helpful comments on the original manuscript. Numerical calculations were done using a modified version of the SOPALE (2000) software. The SOPALE modeling code was originally developed by Phillip Fullsack at Dalhousie University with Chris Beaumont and his Geodynamics group. The numerical experiments presented here are available through contacting the authors.

References

Afonso, J. C., G. Ranalli, and M. Fernandez (2007), Density structure and buoyancy of the oceanic lithosphere revisited, *Geophys. Res. Lett.*, *34*, L10302, doi:10.1029/2007GL029515.

Aldanmaz, E., J. A. Pearce, M. F. Thirlwall, and J. G. Mitchell (2000), Petrogenic evolution of late Cenozoic, post-collision volcanism in western Anatolia, Turkey, *J. Volcanol. Geotherm. Res.*, *102*, 67–95.

Beaumont, C., P. J. J. Kamp, J. Hamilton, and P. Fullsack (1996), The continental collision zone, South Island, New Zealand: Comparison of geodynamical models and observations, *J. Geophys. Res.*, *101*, 3333–3359, doi:10.1029/95JB02401.

Beaumont, C., M. H. Nguyen, R. A. Jamieson, and S. Ellis (2006), Crustal flow modes in large hot orogens, in *Crustal Flow, Ductile Extrusion and Exhumation in Continental Collision Zones*, edited by R. D. Law, M. P. Searle, and L. Godin, *Geol. Soc. London, Spec. Publ.., 268*, 91–145, doi:10.1144/GSL.SP.2006.268.01.05.

Bertotti, G., L. Matenco, and S. Cloetingh (2003), Vertical movements in and around the SE Carpathian foredeep: Lithospheric memory and stress field control, *Terra Nova*, *15*, 299–305, doi:10.1046/j.1365-3121.2003.00499.x.

Bird, P. (1979), Continental delamination and the Colorado Plateau, *J. Geophys. Res.*, *84*, 7561–7571, doi:10.1029/JB084iB13p07561.

Bokelmann, G., and F.-A. Rodler (2014), Nature of the Vrancea seismic zone (Eastern Carpathians)—New constraints from dispersion of first-arriving *P*-waves, *Earth Planet. Sci. Lett.*, *390*, 59–68.

Burchfiel, B. C. (1980), Eastern Alpine system and the Carpathian orocline as an example of collision tectonics, *Tectonophysics*, *63*, 31–62.

Channell, J. E. T., and J. C. Mareschal (1989), Delamination and asymmetric lithospheric thickening in the development of the Tyrrhenian rift, in *Alpine Tectonics*, edited by M. P. Coward, D. Dietrich, and R. G. Park, *Geol. Soc. London, Spec. Publ.*, *45*, 285–302.

Chiarabba, C., and G. Chiodini (2013), Continental delamination and mantle dynamics drive topography, extension and fluid discharge in the Apennines, *Geology*, doi:10.1130/G33992.1.

Conrad, C. P., and P. Molnar (1997), The growth of Rayleigh-Taylor-type instabilities in the lithosphere for various rheological and density structures, *Geophys. J. Int.*, *129*, 95–112.

Csontos, L., A. Nagymarosy, F. Horvarth, and M. Kovac (1992), Tertiary evolution of the Intra-Carpathian area: A model, *Tectonophysics*, *208*, 221–224.

Dahlen, F. A. (1984), Noncohesive critical Coulomb wedges: An exact solution, *J. Geophys. Res.*, *89*, 10,125–10,133, doi:10.1029/JB089iB12p10125.

Dewey, J. F. (1988), Extensional collapse of orogens, *Tectonics*, *7*, 1123–1139, doi:10.1029/TC007i006p01123.

Docherty, C., and E. Banda (1995), Evidence for the eastward migration of the Alboran Sea based on regional subsidence analysis: A case for basin formation by delamination of the subcrustal lithosphere?, *Tectonics*, *14*, 804–818, doi:10.1029/95TC00501.

Downes, H., I. Seghedi, A. Szakács, G. Dobosi, D. E. James, O. Vaselli, I. J. Rigby, G. A. Ingram, D. Rex, and Z. Pécskay (1995), Petrology and geochemistry of late Tertiary/Quaternary mafic alkaline volcanism in Romania, *Lithos*, *35*, 65–81, doi:10.1016/0024-4937(95)91152-Y.

Duggen, S., K. Hoernle, P. Van Den Bogaard, and G. D. Schönberg (2005), Post-collisional transition from subduction to intraplate-type magmatism in the Westernmost Mediterranean: Evidence for continental-edge delamination of subcontinental lithosphere, *J. Petrol.*, *46*, 1155–1201.

Duretz, T., S. M. Schmalholz, and T. V. Gerya (2012), Dynamics of slab detachment, *Geochem. Geophys. Geosyst.*, *13*, Q03020, doi:10.1029/2011GC004024.

Elkins-Tanton, L. T. (2005), Continental magmatism caused by lithospheric delamination, in *Plates, Plumes and Paradigms*, edited by G. Foulger, et al., *Geol. Soc. Am. Spec. Pap.., 388*, 449–461, doi:10.1130/2005.2388(27).

Elkins-Tanton, L. T. (2007), Continental magmatism, volatile recycling, and a heterogeneous mantle caused by lithospheric gravitational instabilities, *J. Geophys. Res.*, *112*, B03405, doi:10.1029/2005JB004072.

Fillerup, M. A., J. H. Knapp, C. C. Knapp, and V. Raileanu (2010), Mantle earthquakes in the absence of subduction? Continental delamination in the Romanian Carpathians, *Lithosphere*, *2*, 333–340, doi:10.1130/L102.1.

Fuchs, K., et al. (1979), The Romanian earthquake of March 4, 1977: II. Aftershocks and migration of seismic activity, *Tectonophysics*, *53*, 223–247, doi:10.1016/0040-1951(79)90068-4.

Fullsack, P. (1995), An arbitrary Lagrangian-Eulerian formulation for creeping flows and applications in tectonic models, *Geophys. J. Int.*, *120*, 1–23, doi:10.1111/j.1365-246X.1995.tb05908.

Girbacea, R., and W. Frisch (1998), Slab in the wrong place: Lower lithospheric mantle delamination in the last stage of the Eastern Carpathian subduction retreat, *Geology*, *26*, 611–614.

Gleason, G. C., and J. Tullis (1995), A flow law for dislocation creep of quartz aggregates determined with the molten salt cell, *Tectonophysics*, *247*, 1–23, doi:10.1016/0040-1951(95)00011-B.

Göğüş, O. H. (2015), Rifting and Subsidence following lithospheric removal in continental back-arcs, *Geology*, *43*, 3–6, doi:10.1130/G36305.1.

Göğüş, O. H., and R. N. Pysklywec (2008a), Mantle lithosphere delamination driving plateau uplift and synconvergent extension in eastern Anatolia, *Geology*, *36*, 723–726, doi:10.1130/G24982A.1.

Göğüş, O. H., and R. N. Pysklywec (2008b), Near-surface diagnostics of dripping or delaminating lithosphere, *J. Geophys. Res.*, *113*, B11404, doi:10.1029/2007JB005123.

Göğüş, O. H., R. N. Pysklywec, F. Corbi, and C. Faccenna (2011), The surface tectonics of mantle lithosphere delamination following ocean lithosphere subduction: Insights from physical-scaled analogue experiments, *Geochem. Geophys. Geosyst.*, *12*, Q05004, doi:10.1029/2010GC003430.

Gray, R., and R. N. Pysklywec (2012), Geodynamic models of mature continental collision: Evolution of an orogen from lithospheric subduction to continental retreat/delamination, *J. Geophys. Res.*, *117*, B03408, doi:10.1029/2011JB008692.

Harangi, S., H. Downes, and I. Seghedi (2006), Tertiary–Quaternary subduction processes and related magmatism in the Alpine–Mediterranean region, in *European Lithosphere Dynamics*, *Mem.*, vol. 32, edited by D. Gee and R. Stephenson, pp. 167–190, Geol. Soc., London.

Harangi, S., M. E. Jankovics, T. Sagi, B. Kiss, R. Lukacs, and I. Soos (2014), Origin and geodynamic relationships of the Late Miocene to Quaternary alkaline basalt volcanism in the Pannonian Basin, eastern–central Europe, *Int. J. Earth Sci. (Geol. Rundsch.)*, doi:10.1007/s00531-014-1105-7.

Hauser, F., V. Raileanu, W. Fielitz, C. Dinu, M. Landes, A. Bala, and C. Prodehl (2007), Seismic crustal structure between the Transylvanian Basin and the Black Sea, Romania, *Tectonophysics*, *430*, 1–25.

Hirth, G., and D. L. Kohlstedt (1996), Water in the oceanic upper mantle: Implications for rheology, melt extraction and the evolution of the lithosphere, *Earth Planet. Sci. Lett.*, *144*, 93–108, doi:10.1016/0012-821X(96)00154-9.
Horvarth, F. (1993), Towards a mechanical model for the formation of the Pannonian Basin, *Tectonophysics*, *226*, 333–357.
Houseman, G. A., and L. Gemmer (2007), Intraorogenic extension driven by gravitational instability: Carpathian-Pannonian orogeny, *Geology*, *35*, 1135–1138, doi:10.1130/G23993A.1.
Houseman, G. A., D. P. McKenzie, and P. Molnar (1981), Convective instability of a thickened boundary layer and its relevance for the thermal evolution of continental convergent belts, *J. Geophys. Res.*, *86*, 6115–6132, doi:10.1029/JB086iB07p06115.
Huismans, S. R., and C. Beaumont (2014), Rifted continental margins: The case for depth dependent extension, *Earth Planet. Sci. Lett.*, *407*, 148–162.
Ismail-Zadeh, A., G. Schubert, I. Tsepelev, and A. Korotkii (2008), Thermal evolution and geometry of the descending lithosphere beneath the SE-Carpathians: An insight from the past, *Earth Planet. Sci. Lett.*, *273*, 68–79.
Ismail-Zadeh, A. T., G. F. Panza, and B. M. Naimark (2000), Stress in the descending relic slab beneath the Vrancea region, Romania, *Pure Appl. Geophys.*, *157*, 111–130.
Jolivet, L., and C. Faccenna (2000), Mediterranean extension and the Africa-Eurasia collision, *Tectonics*, *19*, 1095–1106.
Jolivet, L., C. Faccenna, B. Goffe, E. Burov, and P. Agard (2003), Subduction tectonics and exhumation of high-pressure metamorphic rocks in the Mediterranean orogens, *Am. J. Sci.*, *303*, 353–409.
Jull, M., and P. B. Kelemen (2001), On the conditions for lower crustal convective instability, *J. Geophys. Res.*, *106*, 6423–6446, doi:10.1029/2000JB900357.
Knapp, J. H., C. C. Knapp, V. Raileanu, L. Matenco, V. Mocanu, and C. Dinu (2005), Crustal constraints on the origin of mantle seismicity in the Vrancea zone, Romania: The case for active continental lithospheric delamination, *Tectonophysics*, *410*, 311–323, doi:10.1016/j.tecto.2005.02.020.
Krezsek, C., and A. W. Bally (2006), The Transylvanian Basin (Romania) and its relation to the Carpathian fold and thrust belt: Insights in gravitational salt tectonics, *Mar. Pet. Geol.*, *23*, 405–442.
Krystopowicz, N. J., and C. A. Currie (2013), Crustal eclogitization and lithosphere delamination in orogens, *Earth Planet. Sci. Lett.*, *361*, 195–207, doi:10.1016/j.epsl.2012.09.056.
Leever, K. A., L. Matenco, G. Bertotti, S. Cloetingh, and G. G. Drijkoningen (2006), Late orogenic vertical movements in the Carpathian bend zone—Seismic constraints on the transition zone from orogen to foredeep, *Basin Res.*, *18*, 521–545, doi:10.1111/j.1365-2117.2006.00306.x.
Le Pichon, X., J. Angelier, M. F. Osmaston, and L. Stegna (1981), The Aegean Sea [and discussion], *Philos. Trans. R. Soc. London*, *300*, 357–372, doi:10.1098/rsta.1981.0069.
Lev, E., and B. Hager (2008), Rayleigh–Taylor instabilities with anisotropic lithospheric viscosity, *Geophys. J. Int.*, *173*, 806–814.
Lorinczi, P., and G. A. Houseman (2009), Lithospheric gravitational instability beneath the Southeast Carpathians, *Tectonophysics*, *474*, 322–336.
Lustrino, M., and M. Wilson (2007), The circum-Mediterranean Cenozoic anorogenic igneous province, *Earth Sci. Rev.*, *81*, 1–65.
Magni, V., C. Faccenna, J. van Hunen, and F. Funiciello (2013), Delamination vs. break-off: The fate of continental collision, *Geophys. Res. Lett.*, *40*, 285–289, doi:10.1002/grl.50090.
Martin, M., J. R. R. Ritter, and the CALIXTO Working Group (2005), High-resolution teleseismic body-wave tomography beneath SE Romania: I. Implications for three-dimensional versus one-dimensional crustal correction strategies with a new crustal velocity model, *Geophys. J. Int.*, *162*, 448–460.
Matenco, L., G. Bertotti, S. Cloetingh, and C. Dinu (2003), Subsidence analysis and tectonic evolution of the external Carpathian-Moesian Platform region during Tertiary times, *Sediment. Geol.*, *156*, 71–94.
Matenco, L., G. Bertotti, K. Leever, S. Cloetingh, S. M. Schmid, M. Tărăpoancă, and C. Dinu (2007), Large scale deformations at a locked collisional boundary: Coeval Pliocene-Quaternary differential tectonic movements in the foreland of the SE Carpathians, *Tectonics*, *26*, TC4011, doi:10.1029/2006TC001951.
Merten, S., L. Matenco, J. P. T. Foeken, F. M. Stuart, and P. A. M. Andriessen (2010), From nappe stacking to out-of-sequence postcollisional deformations: Cretaceous to Quaternary exhumation history of the SE Carpathians assessed by low-temperature thermochronology, *Tectonics*, *29*, TC3013, doi:10.1029/2009TC002550.
Morency, C., and M. P. Doin (2004), Numerical simulations of mantle lithospheric delamination, *J. Geophys. Res.*, *109*, B03410, doi:10.1029/2003JB002414.
Mucuta, D., C. Knapp, and J. Knapp (2006), Constraints from Moho geometry and crustal thickness on the geodynamic origin of the Vrancea seismogenic zone (Romania), *Tectonophysics*, *420*, 23–36, doi:10.1016/j.tecto.2006.01.018.
Neil, E. A., and G. A. Houseman (1999), Rayleigh-Taylor instability of the upper mantle and its role in intraplate orogeny, *Geophys. J. Int.*, *138*, 89–107.
Nemcok, M., L. Pospisil, J. Lexa, and R. A. Donelick (1998), Tertiary subduction and slab break-off model of the Carpathian-Pannonian region, *Tectonophysics*, *295*, 307–340.
Oncescu, M. C., V. Burlacu, V. Smalbergher, and M. Anghel (1984), Three-dimensional P-wave velocity image under the Carpathian Arc, *Tectonophysics*, *106*, 305–319.
Pe-Piper, G., and D. J. W. Piper (2006), Unique features of the Cenozoic igneous rocks of Greece, in *Postcollisional Tectonics and Magmatism in the Mediterranean Region and Asia*, edited by Y. Dilek, and S. Pavlides, *Geol. Soc. Am. Spec. Pap.*, *409*, 259–282, doi:10.1130/2006.2409(14).
Platt, J. P., J.-I. Soto, M. J. Whitehouse, A. J. Hurford, and S. P. Kelley (1998), Thermal evolution, rate of exhumation, and tectonic significance of metamorphic rocks from the floor of Alboran extensional basin, western Mediterranean, *Tectonics*, *17*, 671–689, doi:10.1029/98TC02204.
Pysklywec, R. N., and C. Beaumont (2004), Intraplate tectonics: Feedback between radioactive thermal weakening and crustal deformation driven by mantle lithosphere instabilities, *Earth Planet. Sci. Lett.*, *221*, 275–292.
Pysklywec, R. N., and A. R. Cruden (2004), Coupled crust-mantle dynamics and intraplate tectonics: Two-dimensional numerical and three-dimensional analogue modeling, *Geochem. Geophys. Geosyst.*, *5*, Q10003, doi:10.1029/2004GC000748.
Pysklywec, R. N., O. Gogus, J. Percival, A. R. Cruden, and C. Beaumont (2010), Insights from geodynamical modeling on possible fates of continental mantle lithosphere: Collision, removal, overturn, *Can. J. Earth Sci.*, *47*, 541–563.
Ranalli, G. (1997), Rheology of the lithosphere in space and time, in *Orogeny Through Time*, edited by J.-P. Burg and M. Ford, *Geol. Soc. London, Spec. Publ.*, *121*, 19–37.
Ren, Y., G. W. Stuart, G. A. Houseman, B. Dando, C. Ionescu, E. Hegedüs, S. Radovanović, and Y. Shen (2012), Upper mantle structures beneath the Carpathian–Pannonian region: Implications for geodynamics of the continental collision, *Earth Planet. Sci. Lett.*, *349–350*, 139–152.
Rosenbaum, J. M., M. Wilson, and H. Downes (1997), Multiple enrichment of the Carpathian–Pannonian mantle: Pb–Sr–Nd isotope and trace element constraints, *J. Geophys. Res.*, *102*, 14,947–14,961, doi:10.1029/97JB01037.

Royden, L., F. Horváth, A. Nagymarosy, and L. Stegena (1983), Evolution of the Pannonian Basin system: 2. Subsidence and thermal history, *Tectonics*, *2*, 91–137, doi:10.1029/TC002i001p00091.
Russo, R. M., V. Mocanu, M. Radulian, M. Popa, and K. P. Bonjer (2005), Seismic attenuation in the Carpathian bend zone and surroundings, *Earth Planet. Sci. Lett.*, *237*, 695–709, doi:10.1016/j.epsl.2005.06.046.
Sanders, C., R. Huismans, J. D. van Wees, and P. Andriessen (2002), The Neogene history of the Transylvanian basin in relation to its surrounding mountains, in *EGU Stephan Mueller Special Publication Series*, vol. 3, pp. 121–133, Eur. Geosci. Union, Göttingen, Germany.
Sanders, C. A. E., P. A. M. Andriessen, and S. A. P. L. Cloetingh (1999), Life cycle of the East Carpathian orogen: Erosion history of a doubly vergent critical wedge assessed by fission track thermochronology, *J. Geophys. Res.*, *104*, 29,095–29,112, doi:10.1029/1998JB900046.
Sandulescu, M. (1988), Cenozoic tectonic history of the Carpathians, in *The Pannonian Basin: A Study in Basin Evolution*, *Mem*., vol. 45, edited by L. H. Royden and F. Horvarth, pp. 17–25, AAPG.
Schmid, S. M., D. Bernoulli, B. Fügenschuh, L. Matenco, S. Schefer, R. Schuster, M. Tischler, and K. Ustaszewski (2008), The Alpine-Carpathian-Dinaridic orogenic system: Correlation and evolution of tectonic units, *Swiss J. Geosci.*, *101*, 139–183.
Schott, B., and H. Schmeling (1998), Delamination and detachment of a lithospheric root, *Tectonophysics*, *296*, 225–247.
Seber, D., M. Barazangi, A. Ibenbrahim, and A. Demnati (1996), Geophysical evidence for lithospheric delamination beneath the Alboran Sea and Rif-Betic mountains, *Nature*, *379*, 785–790, doi:10.1038/379785a0.
Seghedi, I., H. Downes, S. Harangi, P. R. D. Mason, and Z. Pesckay (2005), Geochemical response of magmas to Neogene-Quaternary continental collision in the Carpathian Pannonian region: A review, *Tectonophysics*, *410*, 485–499, doi:10.1016/j.tecto.2004.09.015.
Seghedi, J., L. Matenco, H. Downes, P. R. D. Mason, A. Szakács, and P. Zoltán (2011), Tectonic significance of changes in post-subduction Pliocene–Quaternary magmatism in the south east part of the Carpathian–Pannonian Region, *Tectonophysics*, *502*, 146–157.
Şengör, A. M. C., M. S. Özeren, M. Keskin, M. Sakınç, A. Özbakir, and İ. Kayan (2008), Eastern Turkish high plateau as a small Turkic-type orogen: Implications for post-collisional crust-forming processes in Turkic-type orogens, *Earth Sci. Rev.*, *90*, 1–48, doi:10.1016/j.earscirev.2008.05.002.
Sperner, B., F. Lorenz, K. Bonjer, S. Hettel, B. Muller, and F. Wenzel (2001), Slab break-off—Abrupt cut or gradual detachment? New insights from the Vrancea region (SE-Carpathians, Romania), *Terra Nova*, *13*, 172–179, doi:10.1046/j.1365-3121.2001.00335.x.
Sperner, B., D. Ioane, and R. J. Lilly (2004), Slab behavior and its surface expression: New insights from gravity modeling in the SE-Carpathians, *Tectonophysics*, *382*, 51–84, doi:10.1016/j.tecto.2003.12.008.
Stern, T., G. A. Houseman, M. Salmon, and L. Evans (2013), Instability of a lithospheric step beneath western North Island, New Zealand, *Geology*, *41*, 423–426, doi:10.1130/G34028.1.
Tarapoanca, M., G. Bertotti, L. Matenco, C. Dinu, and S. Cloetingh (2003), Architecture of the Focsani depression: A 13 km deep basin in the Carpathians bend zone (Romania), *Tectonics*, *22*(6), 1074, doi:10.1029/2002TC001486.
Turner, S. P., J. P. Platt, R. M. M. George, S. P. Kelley, D. G. Pearson, and G. M. Nowell (1999), Magmatism associated with orogenic collapse of the Betic–Alboran Domain, S. Spain, *J. Petrol.*, *40*, 1011–1036.
Ueda, K., T. V. Gerya, and J.-P. Burg (2012), Delamination in collisional orogens: Thermomechanical modeling, *J. Geophys. Res.*, *117*, B08202, doi:10.1029/2012JB009144.
Ustaszewski, K., S. Schmid, B. Fugenschuh, M. Tischler, E. Kissling, and W. Spakman (2008), A map-view restoration of the Alpine-Carpathian-Dinaridic system for the Early Miocene, *Swiss J. Geosci.*, *101*, 273–294.
Valera, J. L., A. M. Negredo, and I. Jiménez-Munt (2011), Deep and near-surface consequences of root removal by asymmetric continental delamination, *Tectonophysics*, *502*, 257–265.
Van der Hoeven, A. G. A., V. Mocanu, W. Spakman, M. Nutto, L. Nuckelt, L. Matenco, L. Munteanu, C. Marcu, and B. A. C. Ambrosius (2005), Observation of present-day tectonic motions in the Southeastern Carpathians: Geodetic results of the ISES/CRC-461 GPS measurements, *Earth Planet. Sci. Lett.*, *239*(3–4), 177–184, doi:10.1016/j.epsl.2005.09.018.
Vaselli, O., H. Downes, M. Thirlwall, G. Dobosi, N. Coradossi, I. Seghedi, and A. Szakacs (1995), Ultramafic xenoliths in Plio-Pleistocene alkali basalts from the Eastern Transylvanian Basin: Depleted mantle enriched by vein metasomatism, *J. Petrol.*, *36*, 23–53.
Wang, H., and C. A. Currie (2015), Magmatic expression of continental lithosphere removal, *J. Geophys. Res. Solid Earth*, *120*, 7239–7260, doi:10.1002/2015JB012112.
Wortel, M. J. R., and W. Spakman (2000), Subduction and slab detachment in the Mediterranean-Carpathian region, *Science*, *290*, 1910–1917.
Zheng, J. P., C.-T. A. Lee, J. G. Lu, J. H. Zhao, Y. B. Wu, B. Xia, X. Y. Li, J. F. Zhang, and Y. S. Liu (2015), Refertilization-driven destabilization of subcontinental mantle and the importance of initial lithospheric thickness for the fate of continents, *Earth Planet. Sci. Lett.*, *409*, 225–231.